Department of Cell and Developmental Biology

University College London

London

Role of complement factor C3 in gastrulation: a novel mechanism of ectoderm epiboly

Isidoro Cobo Rodriguez

November 2014

"Not everything that counts can be counted, and not everything that can be counted counts"
(Albert Einstein)

Acknowledgements

I declare that I personally performed the work described in this thesis, unless otherwise indicated

Abstract

The morphogenetic processes underlying gastrulation are driven through tightly localised cell rearrangements that occur in both ectodermal and mesodermal cells. While some of the cellular movement involved in the involution of the mesodermal cells have been studied in detail, and the movement of ectodermal cells have also been identified, we know very little about what regulates the movement of ectodermal cells during gastrulation. During gastrulation, the ectoderm suffers a dramatic expansion where an initial multilayered tissue becomes single-layered through a process called epiboly. During epiboly of the ectoderm, the superficial layer remains intact, whereas deep cells intercalate between each other, which accounts for an increase in the area of the tissue and the expansion of the superficial layer. However, the mechanism underlying radial intercalation of deep cells during epiboly remains to be unveiled. In zebrafish, radial intercalation of deep cells is thought to partially control the process of epiboly through which the embryo thins and wraps the underlying yolk. Mutants that impair epiboly have been known for some time and resulted from mutations of *half-baked* (which encodes for E-cadhrein). However, the role of Cdh1 in zebrafish epiboly has remained controversial and no detailed characterisation of the role Cdh1 in deep ectodermal cells of *Xenopus* gastrulation has been demonstrated. In this project, we study *Xenopus* epiboly in pursuing of a mechanism that could help us to understand how cell rearrangements are controlled throughout gastrulation.

We have found that at in *Xenopus* gastrulae, the complement component C3a is expressed in the superficial layer superficial layer of the ectoderm, whereas its receptor (C3aR) is distinctly expressed in the deep layer. Complement factors are well characterized components of the immune response, and C3a has been described with chemoattractant activities by binding to it cognate receptor C3aR. We also found that in an *in vitro* assays deep layer cells move towards the superficial layer, showing for the first time chemotaxis of deep cells towards superficial ectoderm. Given the important role of C3a as a chemoattractant, we hypothesised that sensing cells from the deep layer of the ectoderm would be attracted to the C3a-expressing cells, superficial

layer, and that chemotactic movement contributes to radial intercalation of ectodermal cells.

Indeed, in this thesis we demonstrate for the first time that cells from the deep layer of the ectoderm move towards the superficial layer in a process controlled by the anaphylotoxin complement component C3a. We also prove that C3a signalling through C3aR is indispensable for proper gastrulation as embryos lacking C3/C3aR in the ectoderm showed impaired epiboly and thicker ectoderm.

List of contents

List of figures and tables

Abbreviations

- CS: complement system

- PRM: patter recognition molecule

- CRP: C-reactive protein

- MBL: mannose binding lectin

- MASP: MBL associated serine proteases

- FB: factor B

- FD: factor D

- TED: tioester domain

- DAMP: danger associated molecule pattern

- GPCR: G-protein coupled receptor

- HSPC: haematological stem progenitor cell

- CNS: central nervous system

- NPC: neural progenitor cells

- SL: superficial layer

- Deep Layer: deep layer

- RT: room temperature

- IMZ: involuting marginal zone

- NAM: normal amphibian medium

- DFA: Danilchick´s solution

- FN: fibronectin

- MO: morpholino

- ON: overnight

- AP: alkaline phosphatase

- MAB: maleic acid buffer

- CF: complement factors

- CIL: contact inhibition of locomotion

- YSL: yolk syncytial layer

- LMZ: lateral marginal zone

- VMZ: ventral marginal zone

- DMZ: dorsal marginal zone

- ISH: in situ hybridization

- RGC: retinal ganglion cells

- CoA: co-attraction

- AC: animal cap

- C3: complement C3

- FMI: forward migration index

- Blastocoel Roof: blastocoel roof

Part I: Introduction

Chapter 1: Gastrulation

Gastrulation is probably the most dramatic morphogenetic process in early embryonic development. It is a crucial time during embryonic development where cells of the single-layered blastula suffer a substantial rearrangement aiming to form the three embryonic layers: the ectoderm, mesoderm and endoderm. In the next section we will first explain general features of gastrulation and secondly we will describe how gastrulation takes place in different species. Sea urchin gastrulation will allow us to introduce a very simple model for analysing the morphogenesis of a monolayered epithelium. The zebrafish gastrulation will help us to understand how epiboly occurs, as it has been largely studied in this species. As an example of amniotes gastrulation we will use chick, which has important differences with sea urchin, zebrafish and *Xenopus*. Finally, we will explain in more detail *Xenopus* gastrulation because it has been the species used to undertake all the experiments presented in this thesis.

"It is not birth, marriage, or death, but gastrulation, which is truly the most important time in your life". This sentence coined by the pioneering developmental biologist Lewis Wolpert exemplifies very well the actual scope of gastrulation, a crucial process during embryonic development and, therefore, of our life.

The term gastrulation was first quoted by Ernst Haeckel in his work "Biology of Calcaerous Sponges" (1872). Haeckel´s studies of development in calcaerous sponges led him to develop the "*Gastrea* Theory" which proposed that the ancient way of germ layer formation, or gastrulation, involved the invagination of a certain group of cell layers towards a cavity to form the gut. In Haeckel´s words: the gastrula is a "spherical, egg-like or elongated body, which has an inner cavity with an opening (the primordial mouth)". The wall of this cavity is made of two different cell layers: an outer, lighter, ciliated layer, and an inner, darker, unciliated layer; the first is the ectoderm, or outer layer, and the

second is the entoderm or inner (vegetative, nutritive or gastrula) layer in higher animals". Haeckel's observation in Calcaerea was later on supported by photomicrographs of embryos at the same developmental stage by Dr Hammer in 1908.

More than hundred years later, Haeckel's concept of gastrulation has been adapted for other species and, indeed, is regarded as one of the most important phases of embryo development.

Nowadays, we can say that gastrulation is a process that occurs early during embryo development. During gastrulation, a single-layered blastula is reassembled into a three-layered structure called gastrula. These three layers are the ectoderm or external layer, the endoderm or inner layer and the mesoderm, which is formed between the ectoderm and endoderm.

Following gastrulation, each cell layer gives rise to specific tissues and organs in the developing embryo (McGeady, 2004). The ectoderm gives rise to epidermis, the neural crest and other cell types that will eventually constitute the central nervous system. The mesoderm forms the somites, which forms the muscle, the dermis, the notochord, blood and blood vessels, bone, connective tissue, and cartilage of the ribs. Finally, the endoderm forms the epithelium of the respiratory and digestive systems.

Although the timing and molecular mechanism that underlies gastrulation is different in different species, there are common features of gastrulation across all of the organisms that include: a) the formation of a "torus-like" (a structure formed by resolving a circle in three dimensional space) connected surface from a simply-connected (or spherical) surface; b) the differentiation of cells into one of the three cell types (ectoderm, mesoderm and endoderm); c) the generation of a digestive system from a large number of the endodermal cells (Harrison et al., 2010).

Finally, even though gastrulation patterns exhibit enormous variation across all the species, they can be unified by five basic processes involving cell

movement: 1) invagination; 2) involution; 3) ingression; 4) delamination; 5) epiboly (Gilbert, 2010). In the next section I will describe important concepts regarding cell intercalation. In the following section, I will describe very briefly how gastrulation takes place in sea urchin, zebrafish and chick, showing highlighting those processes involving cell intercalation. Finally, I will then focus on *Xenopus* gastrulation, which is the model that has been used to carry out the experiments presented on this thesis.
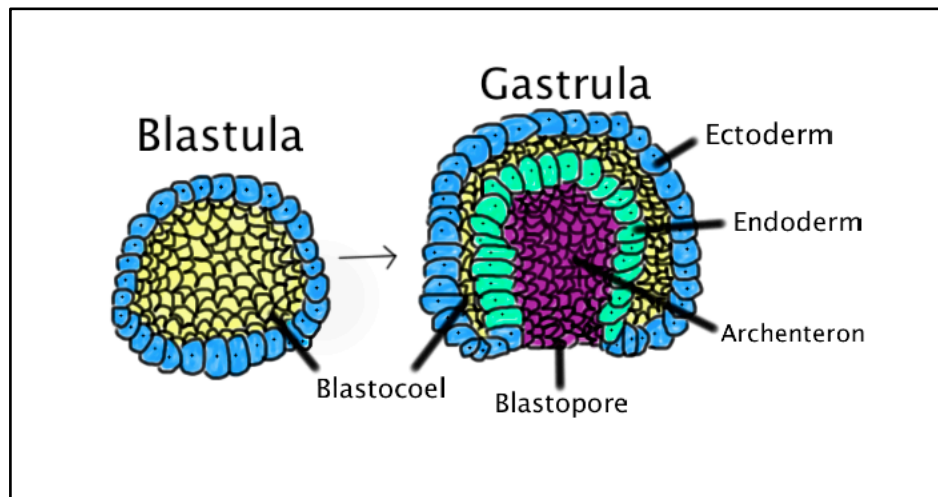
Figure 1. Schematic representation of sea urchin gastrulation. Before gastrulation, almost in all species, embryos are a rounded mass of cells. During gastrulation, there is an invagination of the cells to form a cavity and the specification of the three germ layers.

1.1 Cell intercalation

As it will be described in the following pages, succesful development requires proper movement of cells and proper fater determination. Cell intercalation is one of the movements that orchestrates cellular rearrangement to allow a proper gastrulation and organogenesis, and crucially depends on highly directed exchanges between neighbouring cells, without a change in over cell number (reviewed in Walck-Shanon and Hardin et., 2014). Even though we will mainly focused our attention in early development when the germ layers are organised during gastrulation, this can also occur later during organogenesis if a particular tissue requires an extended morphology.

1.1.1 Mediolateral intercalation

Depending on its direction, cell intercalation can driven various morphogenic movements. First, mediolateral intercalation, in which cells exchange their positions within the same plane. This process underlyes convergent extension movement in a variety of diffent contexts, from the extension of body axis in *Xenopus* and flies during gastrulation, to the extension of epithelial tubes such as the fly trachea or the vertebrate kidney. In other words: "mediolateral intercalation is a specific means by which convergent extension can occur in embryos with bilateral simmetry: neighbouring cells within the same plane exchange places with other along the mediolateral axis to elongate the tissue in the orthogonal axis" (Walck-Shanon and Hardin et., 2014). Multiple other mechanism could drive tissue elongation (Keller et al., 2006), however, cell intercalation is genuine in requiring that the migration and adhesion of many cells are coordinated in space and time to change the shape of a tissue.

For all cell types, succesful mediolateral cell intercalation requires proper polarization of the cells in which rearranging cells quite often lie on the planar cell polarity (PCP) pathway that drives polization of the cells within the same plane of the tissue (Wallingford et al., 2012; Carroll et al., 2012; Tada et al., 2012; Gray et al., 2011; May-Simera et al., 2012). In the next section I will focus in radial cell intercalation for is the movement that the blastocoel roof undergoes during *Xenopus* gastrulation, main focus of this thesis.

1.1.2 Radial intercalation

A second morphogenetic movement is radial intercalation. In contrast to mediolateral intercalation, during radial intercalation cell exchange places throughout the thickness of a multilayered epithelium. As presented above, this movement drives tissue spreading (also called epiboly). As I will describe in next sections, radial intercalation is found during frog and fish gastrulation as

well as during the development skin in frogs (radial intercalation in developmental skin will not be described in this thesis as it goes beyond the scope of this work). It is now clear that radial intercalation is a major driving force for tissue thinning and concomitant epiboly during gastrulation. Radial intercalation movements were firstly described in the animal cap ectoderm of the *Xenopus laevis* embryos (Keller et al., 2003). As it will be described later, in this context, spreading of the animal cap requires cell-matrix interactions with integrins and fibronectin (Marsden and DeSimone, 2001; see gastrulation part of the introduction; see discussion section).

However, in contrast to mediolateral cell intercalation, cells that intercalate radially often do not depend on PCP signals. Moreover, even though there are notable exceptions, in general, different tissue type undergo mediolateral cell intercalation following dinstinctive programmes, with epithelial cells relying on their apical junction and mesodermal cells requiring tractive baso-lateral protrusions. Radial cell intercalation programmes seem to be more context-specific and usually requires non-autonomous signals (reviewed in Walck-Shanon and Hardin et., 2014).

1.2 Gastrulation in sea urchin

Sea urchin embryos have long been used as a model system to analyse the mechanism of gastrulation owing to their transparency, simple organisation and small number of constituent blastomere cells. In sea urchin, gastrulation begins at the vegetal pole, where a particular group of cells (mesenchyme cells) detach and enter the blastocoel. The remaining cells form a vegetal plate and invaginate inwards arranging themselves into a deep and narrow tube that is closed at one end. This tube is the archenteron and eventually becomes the sea uchin´s digestive tract (Figure 1).

Mechanistically talking, before gastrulation, there is a heavy concentration of extracellular material around the ingressing primary mesenchyme cells. On the apical side, cells contact with the extracellular matrix

fibrils. On the vegetal side, cells bind to the hyaline layer (sequence of steps shown in Figure 2). The micromeres originally display a similar pattern of binding for both layers (fibril and hyaline layer). This changes at the onset of gastrulation nonetheless. Whereas some cells retain their ability to tightly bind other cells and the hyaline layer, others lose this ability, while increasing the affinity for proteins found in the blastocoel, such as fibronectin. This change in binding properties is produced by a change in the expression of certain cell surface molecules in the membrane of the cells, and induces the cells to migrate up into the blastocoel (Wessel and McClay 1985).

The remaining cells of the vegetal pole (secondary mesenchyme cells) move then to fill in the gap left by the primary mesenchyme cells in the first phase of the archenteron invagination. The archenteron then extends dramatically. To accomplish this extension, archenteron cells rearrange, flatten, and move over one another flattening themselves. This process, where cells within the archenteron intercalate to narrow the forming tissue, is called "convergent extension" (Figure 3).

At the end, as top cells of the archenteron meet the blastocoel roof, the ingressing cells move into the blastocoel where they proliferate to become the future mouth of the animal.
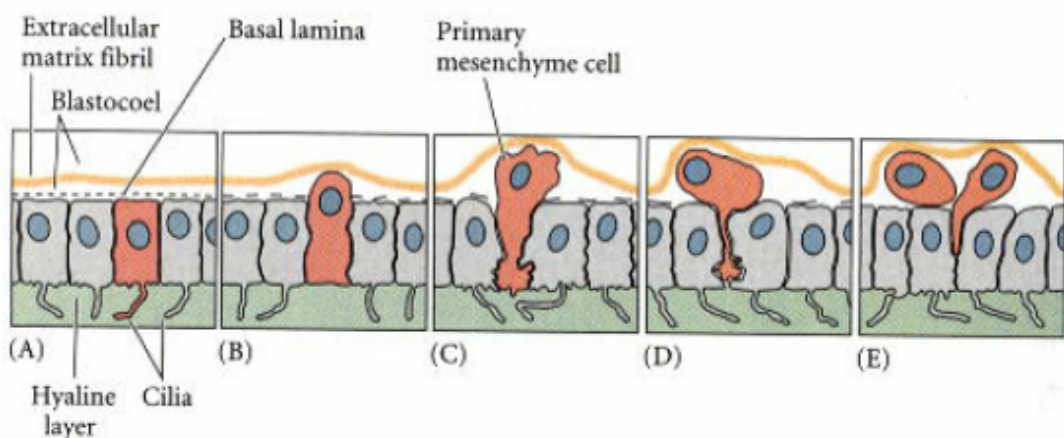
Figure 2. The first step of gastrulation in sea urchin requires a change in affinity for the ECM components. Before gastrulation are strongly attached to the basal hyaline layer and to the neighbouring

cells (A). (B), at the onset of gastrulation, there is a change in binding affinity. Some of the cells (C) lose their attachment to the basal layer to bind molecules at the ECM. This make the cells migrate up towards the bastocoel (D,E). (Modified from Gilbert, 2008).
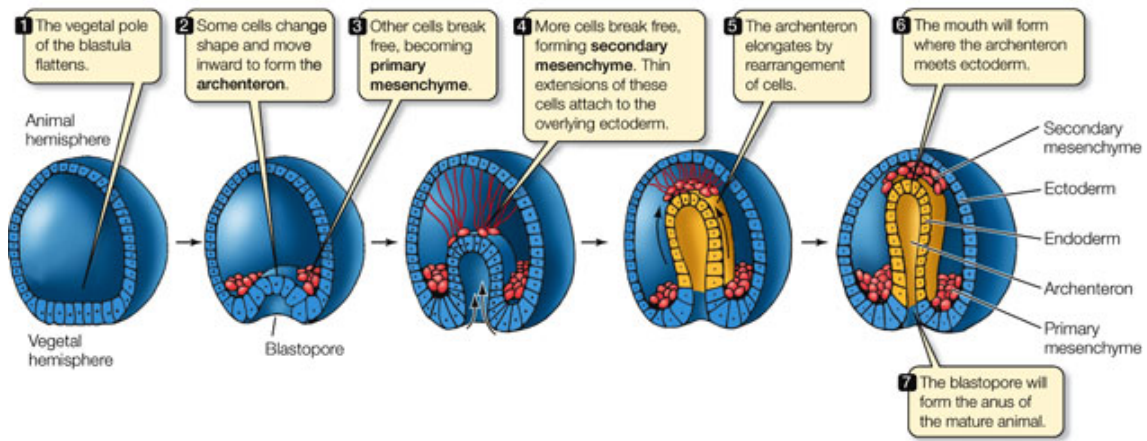
Figure 3. Sea urchin gastrulation. (Modified from Life: the science of Biology, 2007).

1.3 Gastrulation in zebrafish

The blastula stages in zebrafish encompass the midblastula transition to a longer cell cycle and the early phases of epiboly. During this time, the blastomeres become motile and morphogenesis begins. Despite the apparent uniformity of the blastomeres of the mid-blastula stages, tight inspection reveals differences among the cell types (Kane et al., 2005).

The first domain of cells is the yolk cells. In *zebrafish*, divisions are incomplete in the early cleavage stages, leaving the yolk mass undivided. Subsequent divisions separate most of the blastomeres from the yolk mass, however, there is always a ring of cells at the boundary between the yolk and the blastoderm (sometimes termed Wilson cells). At division 10-11 the Wilson cells collapse into the large yolk cell to form a syncitial layer, the yolk cell domain. The second domain is the enveloping layer and corresponds to the cells on the outer surface of the blastoderm. The most outer cells of the enveloping layer will eventually form the first embryo skin, the periderm that will

be later replaced by an ectodermal-mesodermal derived skin. Within the blastoderm, cleavages generate two populations of cells: flattened single epithelial layer forming the enveloping layer (EVL) and rounded, multilayered beneath the enveloping layer, so called the deep layer (DEL) (Warga et al., 1990). Moreover, at the beginning during cycle 10 (Kimmel et al., 1995) the marginal cells undergo a collapse, releasing their cytoplasm and nuclei together into the immediately adjoining cytoplasm of the yolk cell. Thus arises the yolk syncitial layer (YSL), an organ unique to teleosts that makes no contribution to the body of the embryo (Kimmel et al., 1995).

1.3.1 Epiboly initiation

The first phase of zebrafish development encompasses the transition between the sphere to a dome stage (Warga and Kimmel, 1990) and during the next hour a rapid thinning of the blastoderm becomes apparent implying that epiboly is occurring. Epiboly is defined as a cell movement that is characterized as being a thinning and spreading of several cell layers into one single layer of greater extent. During zebrafish epiboly, the deep blastoderm cells move towards the superficial cells (enveloping layer) to intercalate (summarized in Figure 3); however DEL cells do not intercalate outward into the EVL. The deep cells become motile around the midblastula transition, moving in random directions until the onset of epiboly when cells move radially outward (Kane and Kimmel, 1993; Warga and Kimmel, 1990). This notion has been recently tested nonetheless by the experiments performed by Bensch and co-workers (Bensch et al., 2013) in which they demonstrate that there is not directional radial intercalation occurring in zebrafish. Regardless the apparent controversy, although the majority of factors implicated in doming are maternally expressed, zygotic transcription is required, as embryos treated with the transcriptional inhibitor alfa-amanitin fail to dome.

Transcription factors: Pou5f1 and Eomesodermin A

The maternal transcription factors Pou Domain, class 5, transcription factor 1 (Pou5f1, also known as Oct4) and Eomesodermin A are involved in epiboly initiation (Lachnit et al., 2008; Lunde et al., 2004; Reim et al., 2004). The potential role of Pou5f1 in the control of of adhesive and migratory properties of cells during early embryogenesis has been studied in zebrafish (Lachnit et al., 2007). Zebrafish embryos harbouring a mutation in the *pouf1* gene showed a delayed doming with epiboly of the deep cells, EVL and YSL also delayed (Lunde et al., 2004; Reim et al., 2004). Microtubules organization was normal during early cleavage and blastula stages. However, by sphere stage, *pou5f1* mutant embryos showed a defect in microtubules organization, suggesting that the doming delayed could be a consequence of a failure of the microtubules organisation (Lunde et al., 2004; Reim et al., 2004).
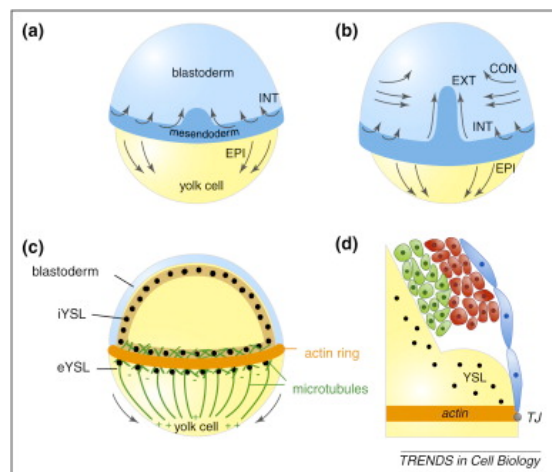
Figure 3 . Schematic representation of gastrulation movements in zebrafish embryos. (a) Dorsal view of an embryo at the onset of gastrulation (6 hpf). At this point, marginal blastoderm cells start to internalize and migrate towards the animal pole (INT, arrows) thereby forming the hypoblast cell layer (blue). Cells that do not internalize form the epiblast cell layer and migrate towards the vegetal pole (epiboly, EPI, arrows). (b) Dorsal view of an embryo at mid-gastrulation stage (8 hpf). Cells move towards the dorsal side of the embryo (convergence movements, CON, arrows) and distribute along the animal-vegetal axis (extension, EXT, arrows). Epiboly and internalization continue until the blastoderm covers the entire yolk cell (EPI). (c) Cross-section of an embryo at the onset of gastrulation (6 hpf) showing the cytoskeleton of the YSL. An actin ring forms within the eYSL at the border between the YSL and the EVL, functioning as a purse-string pulling down the EVL/YSL during epiboly (arrows). Microtubules are present as a dense meshwork surrounding the iYSN and as long parallel bundles originating within the eYSL and pointing towards the vegetal pole. (d) Cross-section at the level of the blastoderm margin showing the different tissue layers undergoing gastrulation movements. YSL with YSN (black); hypoblast (green);

epiblast (red); EVL (blue). The EVL and YSL are connected by tight junctions (TJ). (Taken and quoted from Carvalho and Heisenberg, 2010).

1.3.2 Epiboly progression

The largest increase in the blastoderm surface occurs during epiboly progression. When the enveloping layer has covered around half of the zebrafish embryo (stage called 50% epiboly), the blastoderm expands to engulf the widest part of yolk and shortly after, the deep cell epiboly temporarily ceases as the other movements of gastrulation are initiated (Solnica-Krezel and Driever, 1994). This lag allows the EVL and YSL to internalise and as a result, the deep cells become organised into two layers: the outer, ectodermal epiblast and the inner mesendodermal hypoblast. (The newly formed epiblast forms a thickening termed the germ ring).

Thus, in addition to epiboly, the morphogenetic cell movements of involution, convergence and extension occur, producing the primary germ layers and the embryonic axis (Kimmet et al., 1995). Unlike the initiation of epiboly that occurs independently of convergence and ingression, the epiboly progression is concurrent with involution and convergence (reviewed in Lepage and Bruce 2010).

Cell adhesion molecules

Of the factors implicated in epiboly, the majority are cell adhesion molecules and regulators of cell adhesion and cytoskeletal dynamics. The most studied cell adhesion molecule implicated in epiboly is Cdh1. Initially uniform transcript levels begin to drop denoting higher levels in more superficial cells and lower levels in deeper cells (Kane et al., 2005). Consistent with electron microscopy studies showing that junctional components resembling adherens junctions are present in the EVL, Cdh1 is also expressed in the EVL (reviewed in Lepage and Bruce 2010). The deep cell epiboly defect associated with embryos lacking on *cdh1* is attributed to defects in radial intercalation of the epiblast (Kane et al., 2005; Montero et al., 2005). Moreover, Slanchev and

colleagues (Slanchev et al., 2009) showed that Cdh1 is also required in the EVL for proper epiboly. In this regards, Cdh1 functions redundantly with another transmembrane adhesion protein (EpCAM). A third protein that appears to be required for radial intercalation during epiboly is the Prion protein (reviewed in reviewed in Lepage and Bruce 2010). As in *cdh1* mutants, intercalating epiblast cells failed to flatten against the EVL in *prnprs1* mutant embryos (Málaga-Trillo et al., 2009).

Radial intercalation of deep cells is thought to partially drive the process of epiboly (Kane et al., 2005). As presented earlier on in this thesis, mutants that disrupts epiboly were eventually shown to result from mutations on the *cdh1* gene. Interestingly, even though deep cells are able to intercalate radially to the exterior deep cell layer, they eventually move back towards their original location (so-called reverse intercalation). Until recently, it was thought that a gradient of E-cadherin regulated cell migration from deep to more superficial positions (Kane et al., 2005). This notion has recently turned out controversial nonetheless (Song et al. 2013, see also discussion section). However, even though the support for this graded expression of E-cadherin has been called into question, it is clear that E-cadherin is required for radial cell intercalation of deep cells to properly integrate in their new location resulting in success epiboly (Babb et al., 2004; Arboleda -Estudillo et al., 2010).

Transcription factors: Pou5f1 and Endomesodermin A

The transcription factor Pou5f1 also has also observed to have a role in epiboly initiation (see above), it also has a role in epiboly progression. Marginal EVL cells in *pou5f1* embryos failed to elongate and remain rounded. Pou5f1 has been suggested to regulate the expression of factors involved in regulating microtubules organization during both phases of epiboly (Lachnit et al., 2008; reviewed in Lepage and Bruce, 2010). During progression of the epiboly, Eomesodermin A is critical for radial intercalation and thinning of the epiblast (Bruce et al., 2005). Very recently, the epidermal growth factor (EGF) pathway, has been shown to be downstream of the transcription factor Pou5f1 and required for proper E-cadherin endocytosis and normal deep cell intercalation.

Cytoskeleton

The actin cytoskeleton is mainly involved in the epiboly progression phase (Figure 5). Embryos treated with the actin-depolymerization agent cytochalasin at 50% of epiboly delays epiboly and blastopore closure (Cheng et al., 2004). Strong E-cadherin attachment to the cytoskeleton via α-catenin inhibits blebbing, allowing for efficient radial intercalation (Schepis et al., 2012). E-cadherin-mediated adhesion counterbalances α-catenin- (and ezrin-) mediated blebbing in deep cells (reviewd in Walck-Shannon and Jeff Hardin, 2014). These observations suggest that actin is required for proper progression, completion of epiboly and radial intercalation of deep cells. The Rho family of small GTPases are involved in regulating actin dynamics underlying cell motility. As changes of actin cytoskeleton is important for epiboly, it is not surprising that Rho and other GTPases interacting proteins have been linked to epiboly progression and radial intercalation (reviewed in Ladwein and Rottner, 2008). Work performed in the zebrafish *diaph2* supports the role of Rho in epiboly progression. Diaphanous-related proteins physically interact with Rho to enhance actin nucleation and have been implicated in several cellular processes (for review see Goode and Eck, 2007). In zebrafish*,* Diaph2 have been shown to interact with activated RhoA and Cdc42 (Lai et al., 2008). In embryos injected with *diaph2* MO, actin failed to accumulate at the EVL margin and morphant deep cells displayed a decrease in protrusive activity and slower motility when grafted into *wild type* embryos. Radial intercalation was reduced in *diaph2* MO injected embryos when compared to the sibling controls (Lai et al., 2008). Diaph2 has also been demonstrated to interact with Profilin, a protein that associates with actin monomers and contributes to actin capping (Goode and Eck*,* 2007). When Profilin and Diaph2 levels are synergy reduced simultaneously, embryos showed an impaired epiboly and convergent extension and radial intercalation (Lai et al., 2008).

The maternally and zygotically expressed *chimerin1 (chn1)* plays a unique role in epiboly progression (Leskow et al., 2006). Embryos injected with *chn1* morpholino undergo a quicker epiboly leading to an accumulation of cells

at talibud stages. YSL- specific knockdown of Chn1 led to a similar although milder phenotype, suggesting that Chn1 expression is at least partially required in the yolk during epiboly (Leskow et al., 2006; reviewed in Lepage and Bruce, 2010).
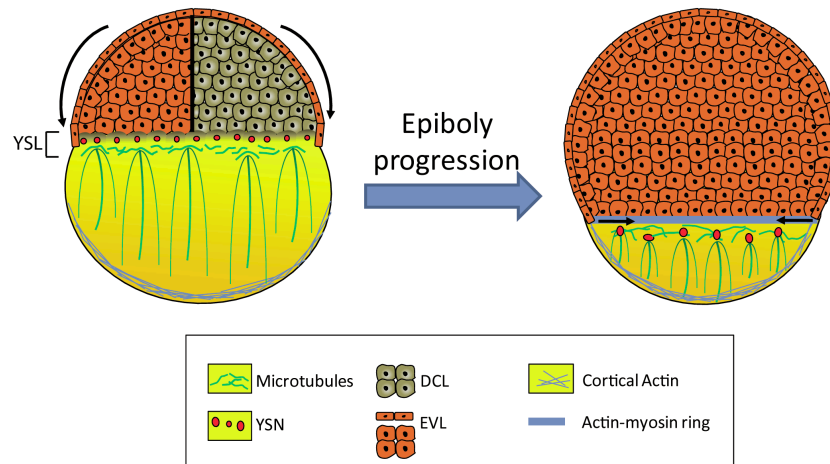
Figure 4. Role of cytoskeleton array during epiboly progression. During epiboly, the blastomeres migrate to envelope the yolk cell. This morphogenic movement is orchestrated by the coordinate changes in the yolk syncitial layer (YSL) cytoskeleton array (mainly composed of actin and microtubules). Parallel microtubule meshwork originating from the yolk syncitial nuclei (YSN) are extending toward the vegetal embryo pole, and participating actively in the epiboly progression. EVL, enveloping layer; DCL, deep cell layer (Taken from Bonneau 2011).

1.4 Gastrulation in chick

In the chick embryo, there is a very tiny white spot on top of the yolk, this very small spot, is where the nucleus is, the non yolky cytoplasm that is where the whole embryo will derive from. The division plane cannot get into the yolky cytoplasm because it is too large; therefore, all the cell divisions occur at that area that is called the blastodisc. As it divides, the blastodisc becomes cellular and is then called blastoderm. Most of the cells of the epiblast remain at the surface of the *area pellucida*, whereas few cells delaminate from the epiblast into the subgerminal area forming the primary hypoblast (see figure 4). Shortly after the delamination of cells from the epiblast, the cells at the most posterior region of the blastoderm migrate anteriorly to join the primitive hypoblast and form the secondary hypoblast. The whole three embryonic layers comes from

the cells of the epiblast whereas hypoblast cells form some portions of external membranes especially of the yolk salk and the stalk that links the yolk sac to the endodermal digestive tube.

The two-layered blastoderm is joined together, and the empty space between the layers of cells forms the blastocoel. (At this point, some people call it the chick blastula, but it is not a real blastula in a real blastula it is a cavity within the cells in the centre of the cellular layers, whereas in the chick the cavity is below the embryo proper). Although the formation and shape of the avian blastodisc differ from those of the amphibian and fish, the spatial relationships are retained among these species. The epiblast colonises the
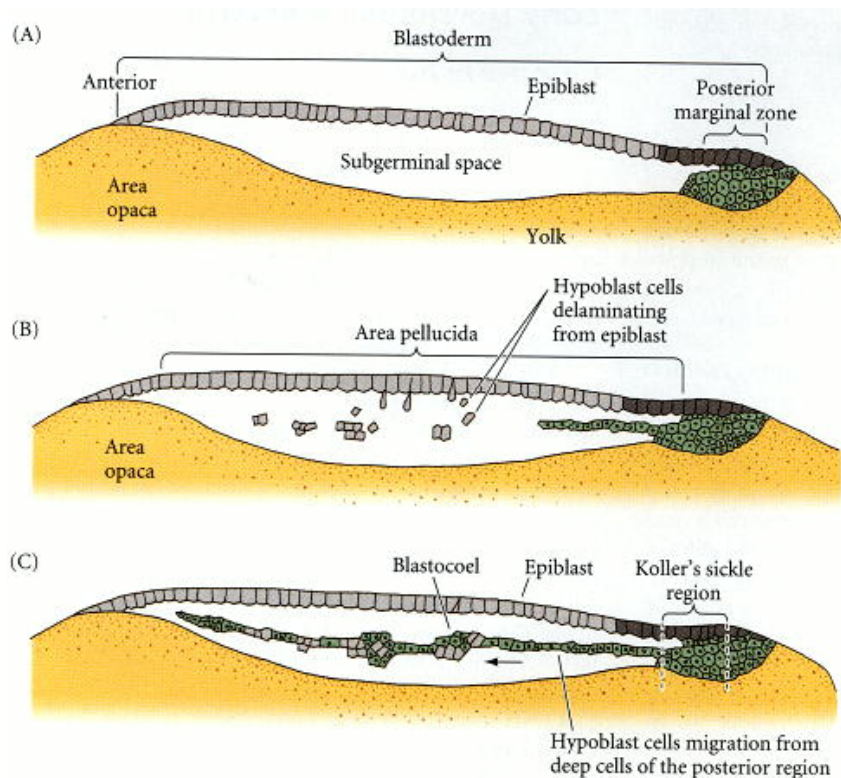
entire yolk. This movement requires the presence of a taut, unbroken *vitelline* membrane which is the substrate on which the epiblast adheres and spreads.

Figure 5. Early phases in the developmental chick. During early phases of chick development, individual cells from the epiblast migrate into the blastocoel to form the primitive epiblast that is joined by cells from the Koller´s´sickle region to become the secondary epiblast . Taken from Gilbert: Developmental Biology Book.

1.4.1 The primitive streak and migration through the primitive streak

Probably, the major structural characteristic of avian, reptilian and mammalian gastrulation is the formation of the primitive streak. Since the chick embryo can be relatively easily manipulated, most of our knowledge about the primitive streak comes actually from avian studies. In the chick, the cells that form the epiblast move as two symetrical rings, known as the "Polonaise" pattern (Graper, 1929; Wetzel 1929). This primitive streak is formed by a combination of two main processes: first, the ingression of presumptive endodermal precursors from the epiblast inside the blastocoel cavity and second the migration of cells from the posterior epiblast towards the center (Vakaet 1984; Bellairs 1986; Eyal-Giladi et al., 1992).

In sea urchin (and others amphioxis) the way the cells move in from the outside to the inside is by pushing into the empty space; in *Xenopus*, the cells crypt inside, first dorsally, then laterally, and finally ventrally. In the chick, however, the cells get in through the blastopore that forms down the midline of the primitive streak. However, how the primitive streak is maintained as a morphologically stable structure despite the fact that the cells are continuously moving remains still unknown (partially reviewed in Voiculescu et al., 2014).

At the anterior end of the primitive streak the Hensen's node is formed. Hensen's node is the functional equivalent of the dorsal lip of the amphibian blastopore (the organizer) and the fish embryonic shield (reviewed in Gilbert, 2008). Cells migrating through Hensen's node pass down into the blastocoel and migrate anteriorly, forming the foregut, head mesoderm, and notochord; cells passing through the lateral portions of the primitive streak give rise to the majority of endodermal and mesodermal tissues (summarized in figure 6). Oppositely to *Xenopus* mesoderm which migrates as a whole layer of cells into the blastocoel, ingression of the mesodermal cells into the blastocoel in chick occurs individually, after undergoing an epithelial-to-messenchymal transition process (Voiculescu et al., 2014). The next cells entering the blastocoel through Hensen's node also move anteriorly, but they do not do so as far ventrally as

the presumptive foregut endodermal cells. Rather, they remain between the endoderm and the epiblast to form the presumptive head mesoderm and the prechordal plate mesoderm (for more detail see Psychoyos and Stern 1996, Gilbert 1998). The following cells in migrating through Hensen's node become notochord cells.
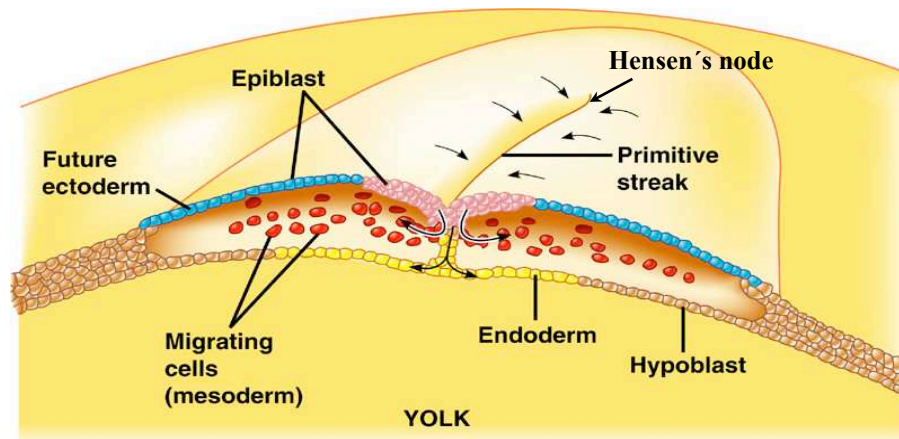
Figure 6. Gastrulation in chick. In the blastoderm, the cells start moving toward the center and form the primitive streak. Next a stream forms down the primitive streak where the cells move in during gastrulation. Cells migrate through the Hensen´s node inside the blastocoel (to form foregut, head mesoderm and notochord) and laterally to form mainly the endoderm and mesoderm. Modified from Gilbert: Developmental Biology Book.

1.4.2 Epiboly of the ectoderm

While the presumptive endodermal and mesodermal cells are moving inwardly, the ectodermal precursors (the outer layer of the epiblast) proliferate and remain outside. Moreover, the ectodermal cells migrate to surround the yolk, a process carried out by epiboly. The wrapping of the yolk by the ectoderm requires the migration of the presumptive ectodermal cells along the whole yolk, by moving underlying the *vitelline* envelope. Within the presumptive ectodermal cells, there is a particular cell population that differs from the other blastoderm cells as they harbour the ability to extend enormous (500µm) filopodia by which they pull themselves and other ectodermal cells around the yolk (Schlesinger, 1958). As it happens for the ectodermal cells in zebrafish (Latimer et al., 2010) and *Xenopus* (Marsden et al., 2010), the chick ectodermal cells attach to

fibronectin, a process that is indispensable for the migration of ectodermal cells. When the ectoderm has surrounded the yolk, the endoderm has replaced the hypoblast and the mesodermal cells have placed themselves in between these two layers, the gastrulation finishes.

1.5 Gastrulation in *Xenopus*

1.5.1 Migration of the involuting mesoderm: radial intercalation and convergent extension.

Among vertebrates, gastrulation has been most largely described in the amphibians, particularly in regard to the cell and tissue movement. *Xenopus* gastrulation centers on the movement of the involuting marginal zone (IMZ) lying at the margin of the floor of the blastocoel. Gastrulation in *Xenopus* begins with what is called the pre-gastrula movement. These movements promote the involution of the IMZ across the blastocoel roof with the formation of a local blastoporal depression, the blastoporal groove and mark the site of initiation of gastrulation.

The outer (apical) surfaces of these cells contract dramatically, while the inner (basal) ends expands. The apical-basal length of these cells greatly increases to yield the characteristic "bottle" shape (described in Gilbert, 2007). The bottle cells are the first cell type that constitutes the dorsal lip of the blastopore, however, as they migrate, the cells that form the dorsal lip are constantly being renewed with other cell types. These bottle cells form progressively first dorsally, then laterally and then ventrally. The next cells in migrating are the cells that will eventually become the prechordal plate (head mesodermal) and the chordamesodermal cells (that will form the notochord).

As the new cells move inside the embryo, the blastocoel cavity is displaced to the opposite side from the blastopore lip. Meanwhile, the dorsal lip extends vegetally as the process of cell involution continues around the blastopore lip. Once the ventral lip is formed, the blastopore forms a ring around

the endodermal cells that remain exposed in the vegetal surface (Gilbert, 2008). The involuting marginal zone is originally composed by several cell layers. Right before the cells start to involute, several layers intercalate to form one single thinner layer.   This process is called radial intercalation and expands the involuting mesoderm toward the vegetal pole.

The superficial layer of the mesoderm spreads out by dividing and flattening. When the deep layer cells reach the dorsal lip of the blastopore, they involute into the embryo and begin a second type of intercalation called convergent extension. During the convergent extension of the mesoderm, several mesodermal cells must integrate into one single narrow stream of cells. The lateral marginal zone (LMZ) and ventral marginal zone (VMZ) also spreads towards the blastopore but a lesser degree. All the processes explained in the last paragraphs are summarised in Figure 9.

1.5.2 Intercalation of mesoderm cells

During *Xenopus* gastrulation, as explained above, in addition to medio-lateral intercalation (Wilson et al., 1991), radial intercalation also occurs in the mesoderm (see gastrulation section). Whereas radial intercalation in the chordamesoderm does not require the overlying blastocoel roof (Wilson et al., 1991), radial intercalation in the prechordal plate mesoderm requires the production of platelet-derived growth factor (PDGF) by the blastocoel roof (Damm and Winklbauer, 2011). Intercalating mesodermal cells extend protrusions towards the blastocoel roof (extended later on the discussion section) which are disrupted upon PDGF abrogation (Damm et al., 2011) suggesting that PDGFa-mediated protrussive activity is required for radial cell intercalation of mesodermal cells.

1.5.3 The ectodermal cells during gastrulation

In contrast to the extensive knowledge about the mesoderm, little is known about the role of the animal cap during gastrulation. During gastrulation, as the Dorsal Marginal Zone involutes, the ectoderm becomes thinner through a process that involves radially directed intercalation of deep cells and flattening of the superficial epithelium (Keller, 1990).

Some authors have proposed that interdigitation between the deep cells occurs during epiboly in the animal cap (Keller, 1990). Superficial cells suffer the stretching force from the deep layer and, as a consequence, they become thinner. Radial interdigitation is then proposed as the cellular mechanism underlying the spreading of the deep region of *Xenopus* cells, during epiboly and extension. Even though these two processes occur in both the ectoderm and mesoderm, there is no clue about what mechanism might be controlling the movement of deep layer cells in *Xenopus* animal cap during gastrulation.

Regions of the gastrula that undergo epiboly, show a decrease in the number of layers of deep cells which carries out rearrangements and temporary changes which account for the stretching of the superficial layer (Keller, 1990). Time-lapse movies show that deep layer cells do not disappear from the deep layer by moving outward into the superficial layer (Keller, 1976; Keller 1980). The outermost superficial layer is a true epithelium while the inner deep cells are free to intercalate (Chalmers et al., 2003). The superficial layer then provides a natural boundary by conforming to the geometry of deep layers (Keller 1978; Keller 1980). Moreover, deep cells cannot migrate more deeply into the interior of the embryo because of the boundary with the blastocoel (Keller, 1980). Also, in the late 70s, vital dye experiments performed by Keller showed that a marked sector of deep region expands as a compact mass of cells (Keller, 1976). These facts strongly suggest that deep cells undergo a local migration movement between one another along the embryo, and that transform several layers of deep cells into one layer of a greater area (Keller 1978; Keller 1990). Such a process of radial intercalation would account for the

spreading of the deep region during extension of the marginal zone and epiboly of the blastocoel roof (Keller, 1980). Furthermore, these data suggest a sequence of changes in deep-cell shape and contact as a cellular mechanism of radial intercalation (Keller 1980). However, the driving mechanism remains still unclear.

The total cell volume remains nearly constant during gastrulation (Tuft, 1965) whereas the extracellular spaces in the regions undergoing epiboly do not seem to change, since they appear as a compact group. This situation is expected for both superficial and deep layer cells, but the amount of thinning in the deep region is higher than what is found in the superficial layer suggesting that spreading of the deep cells should exceed that of the superficial layer (Keller, 1980).

Two periods of thinning have been proposed to explain the change in cell size, shape and arrangement in the course of epiboly in the blastocoel roof. The first involves more than 50% occurs from stage 8 to stage 10+ and it is distributed between the superficial and deep layer. This changes are mainly due to three consecutive rounds of divisions from stage 8 to stage 10+ (figure 7) and this alone is its believed to reduce the linear dimensions of the cells by 45% (Keller, 1990) reaching a minimum of around 3800μm^3. Subsequent with the decrease in the cell shape dimensions, interdigitation of inner cells occurs by stage 10+. Indeed, the thinning and therefore spreading of the deep layer is most pronounced in the period from stage 10 to stage 10+ in which deep region must expand very dramatically in a short time (Keller, 1978). Further correlation studies also suggest that cell interdigitation and deep-to-superficial contact is a coordinated process from 10+ onward (Keller, 1978; Keller 1980). This newly generated area boosts the involuting mesodermal cells and probably contributes to the rapid extension of the dorsal marginal zone during this period (Keller 1980).
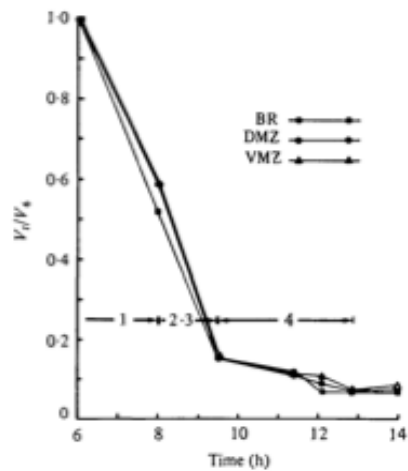
Figure 7. Estimation of the inner deep cell volume of blastocoel roof (BR), Dorsal Marginal Zone (DMZ) and Ventral Marginal Zone (VMZ) across time (Taken from Keller, 1990). The estimations were calculated from the mean apical area and the mean height for the blastocoel roof, dorsal marginal zone and ventral marginal zone respectively. The volume at any time (V_t) was then divided by the volume at 6h (V_6). V_t / V_6 is plotted against time in the y axis. For the blastocoel roof, from the changes in volume it is estimated that about three rounds of divisions takes place over the studied period of time. The numbers plotted over the graph denote the number of cell divisions.

However, even though some of the molecular mechanism underlying epiboly and spreading of deep layer cells have been addressed in mesodermal cells (see beginning of the gastrulation section) we know that epiboly and spreading of the deep cells of the ectoderm differs from what occurs in the mesoderm. In the blastocoel roof, the tendency of cell divisions in the pre-gastrular period to increase the number of cell layers is more than countered by thinning (Keller, 1980). In contrast, the DMZ shows no permanent thinning prior to the onset of gastrulation, and therefore cell division increases the number of cell layers. Spreading and thinning occur throughout the blastula and gastrula stages in the blastocoel roof, but occurs only after the onset of gastrulation in the dorsal marginal zone (Keller, 1978). Moreover, the dramatic change in height/length ratio observed in the deep cells of the ectoderm does not increase to the extent measured in the DMZ (figure 8) and the decrease in the height/ length ratio brings these values below zero (Figure 8). This may be related to the difference between the DMZ and BR in the behaviour of cell spreading suggesting that although there might be some features that accounts for both cell populations, ectodermal cells have a different mechanism to undergo epiboly and spreading.
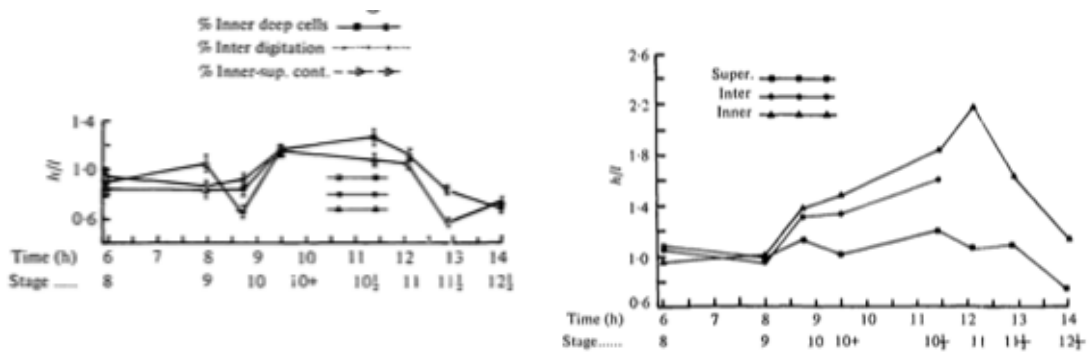
Figure 8. Comparison of the height/length ratio between ectodermal deep layer cells (right) and marginal deep layer cell (left). Taken from Keller, 1980.

In summary, it is clear that the ectodermal cells undergo epiboly and subsequently, spreading in a coordinated manner, that the thinning process in the deep layer cells is much greater that the superficial layer and that deep cells cannot move more inwardly nor intercalate with the cells of the superficial layer. Also, an overview analysis of *Xenopus* gastrulation suggests that ectodermal cells have a different mechanism that mesodermal cell in undergoing epiboly and spreading. Several of the models for the epiboly and spreading of ectodermal deep layer cells that had been initially proposed for zebrafish were then disproven.

Fibronectin and deep cell intercalation

In *Xenopus*, Longo and colleagues proposed a computational model to explain blatocoel thinning and fibronectic assembly during epiboly (Longo et al., 2004). Longo´s model is capable of making some predictions about the BCR thinning process such as cellular rearrangement, the morphology of the tissue layer and the thinning timing. Longo´s model was also succesful in predicting the lateral dispersion of a group of implanted cells. Among the parameters taken into account to build up the model are: that the superficial layers cells do not move towards the deep layer, the superficial layer extends laterally to cover the extending deep layers, the deep layer cells can intercalate into an upper or

lower cell but never into the superficial layer and that the deep cell layer extends as the innermost deep cells intercalate with those that are above them.

Furthermore, the computational model was able to incorporate a role for fibronectin matrix assembly, based on the observation made by Boucoat ´s and Smith´s group (Boucoaut et al., 1984; Smith et al., 1985) and extended by Marsden and colleagues in 2001. In the last study, Marsden and others showed that blastocoelar injection of a fibronectin function-blocking antibody before gastrulation completely blocked the assembly of fibronectin fibril and that fibronectin is required for normal grastrulation. Embryos that lacked the fibrilar fibronectin matrix underwent gastrulation, however these embryos revealed a progressive increase in developmental defects during gastrulation and beyond (Marsden et al., 2001). Among the gastrulation defects, the BCR of embryos injected with the FN function-blocking antibody thickened progressively during gastrulation. The early thinning of the animal cap occurs before fibronectin matrix assembly begins (Keller, 1978) and, therefore, before stage 9 fibronectin has little or no effect on this early phase of epiboly. However, embryos injected with the FN-blocking antibody showed a increase thickening of the animal cap from a layer index of two to a layer index of 4. Interestingly, this later stage of epiboly coincides with the initiation of FN matrix assembly suggesting that even though FN is not required for the initial thinning of the blastocoel roof is required to maintain these cellular rearrangements later during gastrulation. Moreover, this thickening is not due to increased proliferation of deep cells, because no increase in the number of mitotic indices in this cell populations was observed in the absence of fibronectin suggesting a role of fibronectin in regulating cell behaviour in the blastocoel roof.

Combinatorial experiments of superficial and deep layer explants showed that FN can provide a signal that allows deep cells to undergo a intercalative-type movement and that signal acts at a distance from the fibronectin substrate. This suggest that fibronectin plays an instructive role in the BCR thinning process and is required for intercalation of deep ectoderm cells acting at a certain distance (Marsden et al., 2001; Longo et al., 2004). Furthermore, Marsden and colleagues hypothesised that FN matrix assembly are direct results of cell-cell contact in the bottom deep cell layer which causes cells to

remain in the bottom deep cell layer after intercalating to this position (Marsden et al., 2001). However, no molecular explanation of how do cells far from the fibronectin assembly point to intercalate is evidenced. In this thesis we propose a new piece of information that is lacking on Marsden´s model. We show that chemotaxis is indeed a novel mechanistic feature of *Xenopus* ectoderm epiboly.
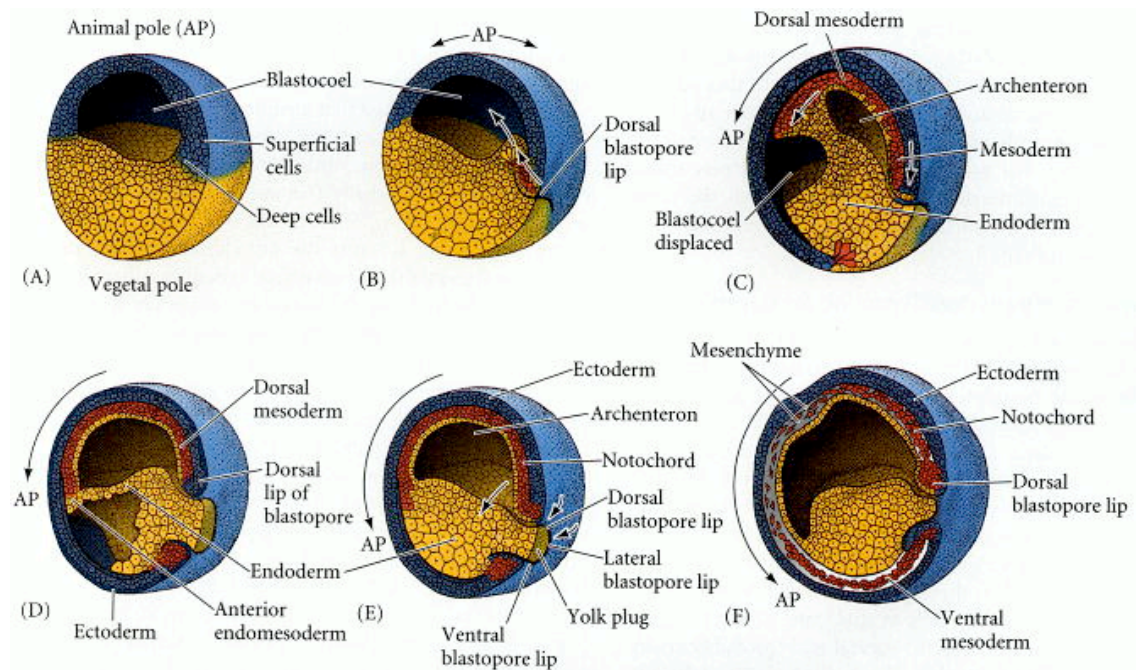
Figure 9. Gastrulation in *Xenopus*. Gastrulation in *Xenopus* starts at the equatorial region of the embryo where the dorsal lip of the blastopre is formed and the involuting mesoderm appears (A, B). As gastrulation proceeds (C) different cell types migrate inwards the embryo and the blastocoel is displaced ventrally. Meanwhile, the archenteron is formed (C) and the three germ layers are specified (D-F). Taken from Gilbert: Developmental Biology Book.
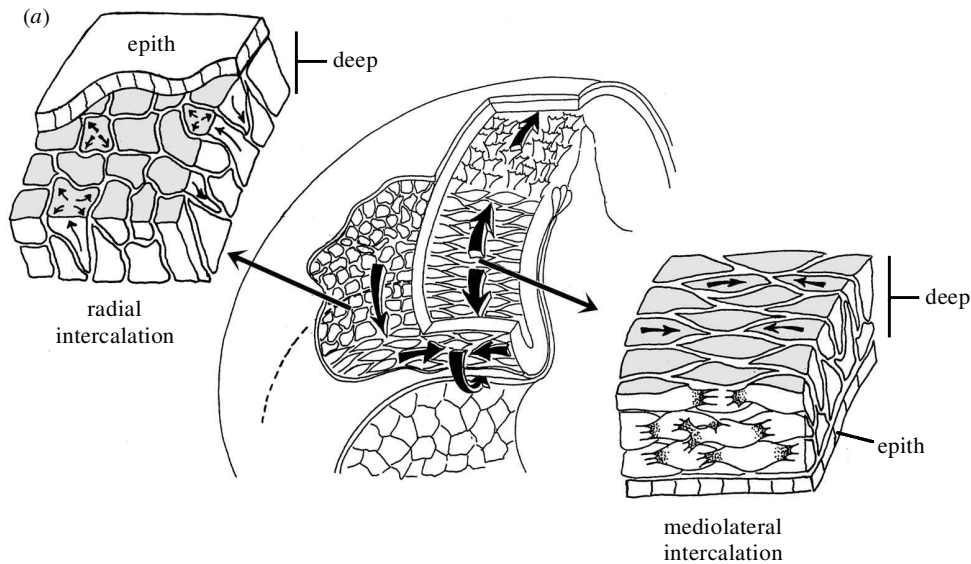
Figure 10. **Mediolateral and radial intercalation.** The expression of radial cell intercalation and mediolateral cell intercalation in the whole *Xenopus* embryo. Radial intercalation consists of several layers of deep cells intercalating along the radius of the embryo (normal to the surface) to form fewer layers of greater area. Mediolateral cell intercalation consists of multiple rows of deep cells intercalating along the mediolateral axis to form a longer, narrower array. The overlying epithelial layer (epith) of the embryo is shown. Taken and quoted from Keller *et al.* 1991

Chapter 2: The complement system

2.1 The complement system in immunity

Our observations and the analysis performed in this thesis suggest that elements of the complement cascade (well known for having a role in immunity), could also play a role in *Xenopus* gastrulation. Therefore I will continue by describing what is known about the complement cascade in the immune system.

2.1.1 Phylogeny of innate and adaptive immune system

Along evolution it is believed that two general systems of immunity emerged: the natural or innate and the acquired or adaptive. The innate immune system is phylogenetically older, already found in some forms of lower multicellular organisms. On the other hand, the adaptive system appeared

around 450 million years ago and is found in all vertebrates except jawless fish (Lambris et al., 1998; Al-Sharif et al., 1997).

In most invertebrates species studied to date, there is no experimental evidence to support the presence of an adaptive immune system. Immune structures gradually developed with the appearance of vertebrate species. The transition to a more elaborated and diverse immune system had been attributed for years to the insertion of a transposon that carries the forerunners of the recombinase genes (RAG1 and RAG2) into the germ line of early jawed vertebrates.

However, among vertebrates, poikilothermic and homeothermic animals have developed different strategies of immune recognition. While homeothermic have expanded their adaptive immune response to a wider network, poikilothermic have mainly relied in the diversification of their innate immune system. Interestingly this diversification has been proposed to allow lower animals to exploit immune system proteins to exert cellular functions outside immunity (partially reviewed in Lambris, 1990). In fact, as we will see in this section, emerging roles for immune system proteins have been recently described.

2.1.2 The complement cascade

Within the innate system, the complement system is one of its oldest components, with its origin in some of the first metazoans. It was discovered a century ago as a heat-sensitive group of proteins that complemented the activity of antibodies in the lysis of bacteria and blood cells. This system was later called "complement system". In the mid 90s, Greenberg and colleagues showed that some complement molecules are present in multiple forms in cold-blooded species (Greenberg et al., 1995; Greenberg et al., 1996).

In the context of immunity, we know that the complement system is a highly regulated cascade that orchestrates immunological and inflammatory

processes, linking up the native with the adaptive immunity. Moreover, by discriminating among healthy host tissue and foreign pathogens, the complement system acts as a very efficient surveillance machinery with a crucial role in resistance to infections and tissue homeostasis, being named as the gatekeeper of immune homeostasis (reviewed in Lambris et al., 2010). The complement system binds very efficiently to the membrane the pathogens thereby promoting an opsonisation and inducing the cell death through the formation of a lytic pore. The complement system can also be activated during the clearance of apoptotic cells in a properdin-initated manner (reviewed in Kemper et al., 2011).

Basically, at the molecular level, the complement system is a finely tuned cascade of proteins that react with one another. A number of complement proteins are proteases that are themselves activated by proteolytic cleavage. The complement system is activated through a triggered-enzyme cascade. In this cascade, an active complement factor that has been previously activated by cleavage of its zymogen, acts as a protease for the downstream component, that is subsequently activated by cleavage and binding to another complement component. Depending on what triggers the initiation of the complement cascade, there are independent ways of activating the proteolytic cascade: the classical, the mannose-binding lectin, and the alternative pathway.

2.1.3 The Classical Pathway

The classical pathway is called the antibody-dependent branch of the complement cascade because it is strongly initiated by immunoglobulins (Ig) clusters. Nevertheless, the wide pattern recognition molecule (PRM) C1q can activate the complement cascade by binding to non-immunoglobulin activators opening the possibility of the complement initiation thorough this pathway in animals lacking on immunoglobulins. Indeed, MacGrath and colleagues suggested that C1q would also bind to C-reactive protein (CRP), fibronectin, SAP, decorin and lactoferrin as well as many polyanions-enriched proteins such as carragenin, heparin, chondroitin sufates, sulfonate and dextran sulphate (MacGrath et al.,2006).

Once formed, the C1q complex recruits the serine proteases, C1r and C1s that will exert its proteolytic function firstly to cleave the complement components C2 and C4. The excision of a small peptide from both C2 and C4 to form C2b and C4b respectively, precedes the formation of the so called, convertase of the classical pathway, C4b2b.

2.1.4 The Mannose binding lectin Pathway

The mannose binding lectin pathway is, mechanistically similar to the classical pathway. It starts with the recognition and attachment of Manose Binding Lectin and ficolins to carbohydrate patterns on the cell surface triggered to activate the complement cascade. Whereas the classical pathway is triggered through the binding of C1q to the cell surface, the MBL pathway is initiated through the binding of mannose-binding lectin to mannose, glucose (and other carbohydrates) as well as glycoproteins present in the membrane of bacterial pathogens.

MBL binds MBL-associated serine proteases, MASP-1 and MASP-2, which share structural similarity with the key molecules C1r and C1s of the classical pathway. Of these, MASP-2 cleaves both C2 and C4 whereas MASP-1 can only cleave C2 and, therefore, can support the pathway once it is initiated, thereby rising the efficiency of convertase formation.

After C4 and C2 are cleaved into C4b and C2b respectively, the same C3 convertase of the classical pathway is formed and C3 is further converted to C3a and C3b. As it will be shown in following paragraphs, C3b acts as an opsonin molecule, being deposited on the target cells, and thereby activating downstream complement components. On the other hand, C3a as a potent chemoattractant during complement activation and contributes to tissue homeostasis and regeneration, counterbalancing the effect of the lytic pore formed by the downstream complement components (schematic representation

of the early events in activation of the complement cascade by the classical and manose-binding lectin is shown in Figure 12) .
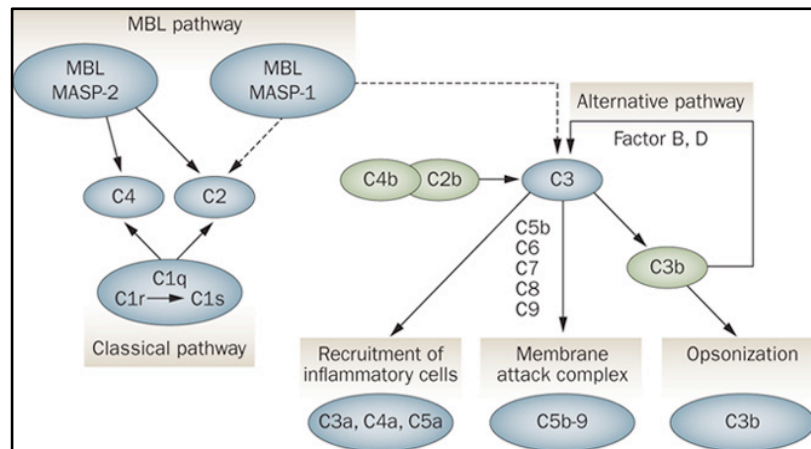
Figure 11: Early events in activation of the complement activation through the MBL and Classical pathways. In the MBL and classical pathways, the complement cascade requires an initiating molecule that binds to the foreign cell membrane, thereby promoting the deposition of downstream components. Note the similarity of activation in both pathways. Modified from Allan Flyvbjerg (Nature reviews, 2006).

2.1.5 The alternative pathway

Despite its name, the alternative pathway consists of three overlapping processes that represent up to 80-90% of total complement activation even though it is initially triggered by the classical or the Manose Binding Lectin pathways.

The first process is called "tick-over" and allows the complement system to probe constantly all the cells of the organism. In its native form, C3 is relatively inert, exposing few epitopes and ligands to undertake conformational changes. Nonetheless, a very small fraction of C3 is attacked by small nucleophiles such as water or ammonia, thereby dehydrating C3 into $C3(H_2O)$ (Pangburn et al., 1983). The resultant molecule is extremely similar in conformation to C3b and can form a complex with Factor B (FB) which is used as substrate for Factor D (FD) protease. Then, FD removes a small peptide from FB (Ba) leaving the remaining FB protein (Bb) bound to C3b in order to form the alternative pathway C3 convertase, C3bBb.

In summary, the alternative pathway differs from the classical and the MBL pathways in the sense that the alternative pathway can be activated due to the spontaneous cleavage of C3 and the intrinsic ability of C3 to bind a wide range of activator antigens. Nevertheless, even though C3b shows some preference for binding to certain residues, it is not able to display an accurate discrimination between host and foreign tissues and, therefore, the complement cascade requires the activity of some regulatory proteins to continue the amplification of the cascade.

Activated C3b will gradually lead to the formation of convertases that contain an additional C3b molecule, C4b2b3b for the Classical Pathway and the Mannose Biding Lectin pathway and C3bBb3b for the AP. The addition of a new C3b shifts the specificity of the enzyme for the substrate from C3 to C5.

During the activation and amplification steps, C3a and C5a molecules are constantly released and trigger a potent inflammatory response by binding to their corresponding G-Protein-Coupled-Receptor (GPCR). Anaphylotoxins C3a and C5a are powerful chemoattractants whose gradient is used by the inflammatory cells to reach the complement activation point (Hartmann et al., 1997). (An overview representation of the complement activation is shown in Figure 13).

2.1.6 C3 proteolytic products and C3aR

C3 is the convergence point for the three pathways that can trigger the complement activation. It consists of one beta and one alpha chain linked by a disulphide bridge and by non-covalent forces. C3 contains 13 domains; it has eight domains with a fibronectin-type-3-like core, which in analogy to the immunoglobulin domain are referred to as Macroglobulin domains. It also contains an anaphylotoxic domain (ANA which will be eventually excised from C3 to become C3a), a CUB domain (that has been proposed as a putative

bridge between MG7 and MG8 domains), a linker (LNK) domain and a carboxy-terminal domain called C345, with a netrin-like fold. (the whole C3 structure is summarized in Figure 12a)
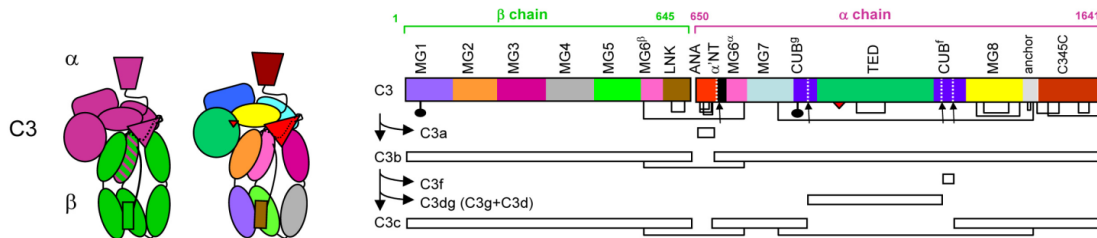
Figure 12: Domains of h-C3 protein (modified from Jansen et al., 2006) and cleavage sites . Schematic representation of the different domains of C3. Colour scheme in the sequence diagram matches that in the arranged structure shown in the left half of the figure.

C3 contains a highly reactive TED moiety that is protected from reacting with the water or other nucleophiles by a hydrophobic pocket between MG8 and TED itself. A single cleavage of C3 removes the ANA domain C3a, inducing a strong conformational change that activates C3b with an exposed and highly reactive TED, as well as other binding sites. In fact C3a removal weakens the interaction between TED and MG8, allowing TED to swing out from the buried initial state (Jansen et al., 2006). On the other hand, similar although much slower, conformational changes occur when C3 is spontaneously hydrolysed.

As indicated before, native C3 is quite inert, showing almost no reactivity with any of the other complement factors and it is unable to form the C3 convertase. Nevertheless, by exposing its reactive TED, C3b becomes activated and displays a tremendous ability to bind cell surfaces and, most importantly, other complement factors such as Factor B and D, thereby generating C3 convertases, promoting C3b production, and subsequently allowing the activation of downstream components.

2.1.7. C3a works as a chemoattractant

Therefore, activation of C3 is the central step in the activation of the complement cascade and it happens through the activation of a TED, which is buttressed inside the C3 native protein by the presence of C3a This activation has very important implications for convertase formation and regulation. However, based on this structural notion, C3a had been considered as a residual domain of C3. This concept has been challenged after the discovery of key cellular processes that are controlled by C3a/C3aR axis. In fact, C3a signalling through C3aR is essential for a proper inflammatory response during complement activation. Together with the peptides of bacteria origin and some cytokines (such as the C, CC, CSC and interleukins) the complement components C3a and C5a orchestrates the chemotactic movement of immune cells during inflammatory response. In 1995 Daffern and colleagues show that C3a acts as a chemoattractant for eosinophils but not for neutrophils (Daffern et al., 1995). After that, in 1997, Zwirner and colleagues found that the mouse macrophage cell line J774 migrate along a concentrated gradient of C3a but not C3adesarg (a peptide that lacks the C3aR binding domain) suggesting that C3a is a potent chemoattractant for this macrophage cell line and its chemotaxis is dependant on its binding to C3aR (Zwirner et al., 1997).

Also, in 2004 Gutzmer and co-workers demonstrated that in human monocyte-derived dendritic cells, when C3aR is upregulated upon interferons treatment (but not with other *stimuli* such as LPS or CD40 ligand), cells are chemoattracted to a C3a source in Boyden chamber chemotactic assays (Gutzmer et al., 2004).

However, C3a not only promotes chemotaxis of inflammatory cells. In 2009 Schraufstatter show that C3a is also a chemotactic factor for human mesenchymal stem cells (Schraufstatter et al., 2009). Chemotaxis was specifically mediated by C3aR as shown by the inhibitory effect of the specific C3aR inhibitor SB290157 on C3a-mediated chemotaxis. Moreover, this inhibition could not be due to any specific effect of the inhibitors as bFGF-mediated chemotaxis was not impaired when cells were treated with SB290157.

As expected because of the GPCR nature of the C3aR, C3aR response was coupled to G_i as noted by the blockage of migration upon presence of pertrussis toxin (a molecule that prevents G protein to bind GPCR). However, the most intriguing observation that Schraufstatter´s work show is the demonstration that inactivation of the C3aR in human mesenchymal cells causes nuclear translocation of the C3aR.

Very recently, Hartmann and co-authors have shown by using Boyden chambers assays that C3a can also stimulate chemotaxis of human mast cells (Hartman et al., 2014). The migration was impaired when the cells were treated with the C3aR inhibitor SB290157 or in the presence of the pertrussis toxin, supporting the fact that C3a-promoted chemotaxis is dependant specifically on C3aR and GPCR activation. Finally, C3a can also promote chemotaxis indirectly by enhancing the activity of other inflammatory cytokines such as CXCL12 (Honczarenko et al., 2005).

Figure 13: Detailed view of complement activation, regulation and amplification during its immunological role. An intricate network of membrane-bound and soluble factors modulates the activation and amplification of the cascade. During its role in immunity, several cell types are involved in the complement-meditated clearance of unwanted cells. Among all the cascades and process, three of them are noteworthy: a, the constant activation (tick-over) of the alternative pathway that constantly probes the cells in pursuit of what needs to be cleared; b, the amplification mediated through stabilization of C3 convertase by properdin; c, the potential role of other molecules in initiating the complement activation (extrinsic pathway). (Taken from Ricklin et al., 2010)

2.2 Non immunological roles of the complement system

It is well established that the complement system is an integral member of the innate mechanism of immunity, in which C3 plays a key role. However, recent findings have deeply reshaped the understanding of the complement system. Indeed, besides its original role in immunity, the complement system is also involved in other processes such as mobilisation of hematopoietic stem-progenitor cells (HSPCs), tissue regeneration, lipid metabolism, angiogenesis, wound healing, and reproduction (Mastellos, D. & Lambris, J. D, 2002). Thus, the historical notion of the complement system as a supportive system for the immune response has been deeply challenged.

2.2.1 The complement system during animal development

Among all the processes outside immunity, animal development is probably the field in which most of the evidences for a distinctive role of the complement system has emerged (partially reviewed in Ricklin et al., 2010 and Leslie and Mayor., 2013). In fact, among all the complement proteins, C3 is the most versatile and multifunctional molecule described to date, having evolved structural characteristics that allow it to interact with more than 20 different proteins (Lambris et al., 1998). Interestingly, C3 is a very ancient molecule that emerged 700 million years ago, long before the appearance of the immunoglobulins (Sahu and Lambris, 2001) suggesting additional roles for C3 outside immunity. Moreover, C3 is expressed in the regenerating limb blastema cells of urodeles suggesting a role for C3 in regeneration (Del Rio-Tsonis et al., 1998), a process where cell movement is required. In the current section I will explain in more detail our present understanding of how complement system contributes to some aspects of animal development. I will then focus on the role during *Xenopus* embryonic development for has been the animal model used during this thesis.

2.2.1.1 Synapse elimination

Certain sites of the human body are able to tolerate the presence of antigens without eliciting any inflammatory immune response, a situation that is called "immune privilege". Immune privilege is regarded as an evolutionary mechanism that protects vital structures against any event of inflammation that could severely compromise survival. Among other tissues, the brain was thought to be an immunologically privileged organ based on the low expression of immune system proteins on the central nervous system (CNS) cells.

This notion has been challenged nonetheless. Thanks to high sensitivity methods of RNA and protein detection it is now clear that some inflammatory cytokines, complement components and other proteins of the innate immunity such as Major Histocompatibility Proteins are expressed in the nervous system and are important during central nervous system development (Morgan and Gasque, 1996; Johnson et al., 1994).

The classical pathway of the complement system in particular has been demonstrated to take part in synapse elimination in mice. At birth, the mouse brain contains excessive amount of neural connections between the dorsal lateral geniculate nucleus (deep layerGN) and the retina. All three C1q chains and C3 are expressed in the neurons that form these connections; the retinal ganglion cells (RGCs). Neighbouring astrocytes activate C1q and C3 expression. In the mechanism proposed by Stevens and colleagues (Stevens et al., 2007), C1q would tag the cells to be eliminated through the further deposition of downstream complement component C3. They also observed that C1q becomes aberrantly upregulated in a mouse model of glaucoma prior to observable neurodegeneration, suggesting that the complement cascade also mediates synapse loss in glaucoma and other CNS neudegenerative diseases.

2.2.1.2 Tissue regeneration

Regeneration is a highly regulated process in which cells must recognize environmental signals and respond in a proper way. As indicated earlier on, C3a and C5a are involved in regeneration of adult tissues. The liver of mice lacking C5, for instance, displays an impaired recovery after damage (Kimura et al., 2003). Furthermore, authors found that this regenerative function of C5 occurs via the proteolytic fragment C5a and C3a, rather than the formation of the MAC (C5b-C9). This suggests that the so-called residual complement components C3a and C5a participates in regeneration of mouse liver independently of the downstream components member of the membrane attack complex.

In lower species, Kimura and colleagues (Kimura et al., 2003) found that C3 and C5 are involved in regeneration of urodele newt limbs. This description of a distinct expression profile of complement proteins in regenerative urodeles tissues constitutes the first systematic effort to discriminate the involvement of complement cascade in regenerative processes in lower vertebrates (Kimura et al., 2003). Very recently, Haynes and colleagues identified that complement C3a is sufficient to induce complete regeneration of the embryonic chick retina through the activation of Stat3 downstream genes IL6, IL8 and TNF-a (Haynes et al., 2013).

2.2.2 Complement System during embryonic development

2.2.2.1 Collective cell migration

Previous work from our lab demonstrated that several complement components, such as C3, C2, C4, CFH, CFI, CFB, and CFD are expressed in the migratory neural crest, suggesting, a role of the complement cascade during migration of the neural crest (Figure 6). However, in order to understand how the complement system interplays with the neural crest as they migrate, we must first analyse neural crest migration as a collective group. Collective cell migration is defined as a coordinated movement of cells and is involved in a

number of processes in different species: migration of the nerual crest cells in many vertebrates, lateral line development in zebrafish (Breau et al., 2013), and border cell migration in Drosophila (McMahon et al., 2008).

Due to their mesenchymal nature, the NC cells form transient cell-cell junctions with other neural crest cells within a cluster. They also suffer a form of repulsion called Contact Inhibition of Locomotion -CIL- (Carmona-Fontaine et al., 2010) during which cells collide, cease their migration, repolarise and change its direction. How, then, can a population of cells that is normally repelled migrate as a group? Partially, the answer to this question comes from the mutual cell attraction between neighbouring cells, the countervailing co-attraction (CoA) effect. C3a acts as a co-attractant during *Xenopus* NC migration (Carmona-Fontaine et al., 2012). Migratory NC cells produce both C3a and C3aR, which are indispensable for a proper neural crest migration by promoting mutual cell attraction between neural crest cells. C3a-C3aR mediated signalling outweighs the forces of CIL that drives NC cells far from each other. Depletion of either C3a or C3aR inhibits NC cells migration by promoting enhanced cell dispersion and decreased cohesion of the cell group.

More than a century after the significance of the human complement system was recognised, recent studies have made us to realise that its function extends far beyond its historical immunity roles (Ricklin et al., 2010). The findings of the role of the complement system during synapse elimination (Stevens et al., 2007), urodele newt limbs regeneration (Kimura et al., 2003) suggest a role of the complement system during animal development. The early expression pattern of C3 together with the fact that C3a regulates *Xenopus* neural crest migration (Carmona-Fontaine et al., 2010) led us to study the role of complement component C3 earlier stages during *Xenopus* embryonic development, particularly regulating cell movement during *Xenopus* gastrulation.
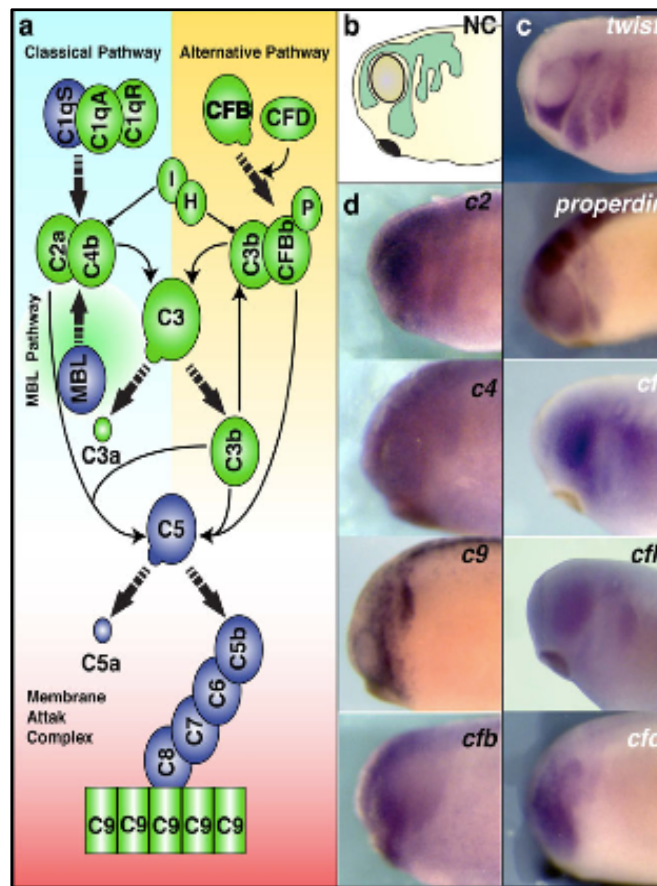
Figure 14: **Several components of the complement system are expressed in the migratory neural crest**. a, visual representation of complement cascade. Green components denote the components that, so far, have been found to be expressed in the migratory neural crest. b, schematic representation of migratory neural crest. c, expression of a classical neural crest marker, Twist. d, expression pattern of some complement components. (Figure taken from Carlos Carmona´ s thesis)

In immune cell homing, the complement is a highly regulated cascade that triggers the formation of a pore on the target cell and the production of proteins with chemotactic capacities (see section 2 of the introduction). Among others, C3 is cleaved to produce C3a, a small anaphylotoxin peptide that binds to C3aR and triggers chemotaxis. Previous studies focusing on neural crest cell migration in *Xenopus laevis* revealed that complement factor C3a is important for morphogenesis early during embryonic development, and this role is independent of its function in the immune system (Carmona-Fontaine et al., 2012). These findings raise the possibility that C3 signalling might control tissue morphogenesis in other contexts.

We explored this notion, in the pursue of finding new cellular processes during *Xenopus* embryonic development whose mechanism involves cell

migration and could be regulated by C3/C3aR. In particular, given the role of complement C3 in regulating cell movement and the importance of local cell arrangement during epiboly of the ectoderm, we examined the expression of C3 and its cognate receptor C3aR in early embryos at stages of blastocoel roof epiboly. In situ hybridisation and Western Blot assays would allow us to recognise the expression pattern of C3 and C3a/C3aR respectively in the different cell populations of the blastocoel roof. In this regards, we aim to understand how complement-mediated cell interaction in ectoderm cells during *Xenopus* gastrulation. To address this, loss of function experiments using specific C3 and C3aR antisense morpholino would help us to understand whether C3 and C3aR are required for ectodermal epiboly *in vivo*. *In vitro* experiments using explants from the different cell types of the BCR will allow us to study whether there is some clue within the BCR that drives the movement of the ectoderm cells (C3a/C3aR involvement could be then tested). Moreover, given that the prevailing model to explain epiboly in zebrafish is based on differential adhesiveness between interior and exterior epiblast cells mediated by E-cadherin, we could also test whether cell-cell adhesion is also the molecular model underlying epiboly of the BCR.

— Part II: Material and Methods

2.1 Obtaining *Xenopus* embryos

To obtain *Xenopus laevis* embryos, mature females must be pre-primed with a subcutaneous injection of 100 units of serum gonadotrophin (Intervet) 4 to 7 days before stimulation of ovulation. Stimulation was performed 12-15 hours prior to fertilisation, by injecting 500 units of choronic gonadotrophin (Intervet). To collect oocytes laid overnight, the animals were then placed in Egg-laying medium (Ca_{2+} free, see solution section for recipe). For *in vitro* fertilisation, a small piece of testis was mixed with the oocytes in a dry Petri dish. To obtain the testis, adult male *Xenopus* were terminally anaesthetised in a solution of 0.5% Tricaine (3-amino benzoic acid ethylester) and the organs were dissected and stored in Leibovitz L-15 medium (Invitrogen) at 4ºC. Cortical rotation occurs after 20-40 minutes, at which point the dish was flooded with 1/10 NAM. At the 2-8-cell stage (depending on stage of embryo injection see below), the jelly was removed from the embryos in a solution of 2% L- cysteine (pH8.2) and the embryos were cultured in normal amphibian media (NAM) 1/10. Embryo staging was assessed according to Nieuwkoop and Faber (Nieuwkoop and Faber, 1967)

2.2 Morpholino and mRNA microinjection

Morpholino and mRNA microinjections were performed using a Narishige IM300 Microinjector under a Leica MZ6 or a Nikkon SMZ645 dissecting microscope. Borosilicate capillaries (Intrafil, 0100106) were pulled to make thinneedles with a Narishige PC-10 puller. The puller was set to the two-step mode with both steps adjusted at the 69,5% of its capacity. The needles were then calibrated using an eyepiece graticule to inject 5nl or 10nl. Dishes filled with ficoll were used to inject *Xenopus* embryos at the 8-cell stage and the embryos were cultured in ficoll for 6-12 hours to let them recover after the injection. The ficoll was then washed out and the embryos were incubated on 1/10 NAM.

The embryos were peeled on 3/8 NAM to promote a fast recovery after the incision made to peel the embryos and incubated for half an hour at RT or until the embryos healed. Once no sign of injury was observed, the embryos were moved to a new dish with 1/10 NAM.

2.3 Deep layer and Superficial Layer explantation

To isolate Deep Layer and Superficial Layer from the ectoderm, three incisions were performed in the animal cap of stage 10-12 embryos that were previously peeled. Upon incision and opening the animal cap gets exposed, with the Deep Layer and Superficial Layer. Deep Layer was then shaved from the Superficial Layer. Superficial Layer was then taken when no Deep Layer cells were observed in the tissue. All the procedure was performed on 3/8 NAM. A summarising diagram is shown in Figure 3.1f.

2.4 Deep Layer, Superficial Layer and Neural Crest culture in plastic

Fibronectin-coated plastic dishes were used for deep layer, superficial layer and neural crest culture. Sterilised plastic dishes were incubated for one hour at 37ºC with a solution of fibronectin (FN) 10µg/mL (from Sigma) diluted in PBS. Three five-minutes washes with PBS were performed to remove fibronectin traces before incubating the dish with PBS/BSA for 15-30 minutes. After that, dishes were washed again three times with PBS and then incubated with Danilchick´s solution (DFA).

Dissection of the Deep Layer and Superficial Layer was carried out as described in 2.3. Once removed, Deep Layer and Superficial Layer explants were transferred to the fibronectin-coated plastic dishes containing DFA and kept stationary until the cells attached to FN. Attachment to the substrate was tested by shaking gently the plastic dish. When the explants were attached to

FN, the dish was completely filled with DFA, closed (making sure no air bubbles remained inside) and inverted for time-lapse movies analysis.

Neural Crest cells were dissected from embryos at the stage 17 as described previously (Alfandari et al., 2003; Carmona-Fontaine et al., 2008). As it was done for Deep Layer and Superficial Layer, dissection the NC cells was performed in 3/8 NAM and, once removed, they were transferred to a FN-coated dish filled with DFA. NC cells were kept stationary at room temperature until they attached.

2.5 Deep Layer, Superficial Layer and Neural Crest culture in plastic

To measure the cell-cell substrate adhesion, cell cultures were performed as normal but flipped after 2 hours. Then the percentage of explants that remained attached was counted. Experiments were done in triplicate. Differences of cell-cell adhesion were determined using a cell-sorting assay described in (Ninomiya et al., 2004) with some minor modifications. The main modification was that cells from different conditions were separated using a calcium-magnesium free DFA medium instead of the 50%-calcium magnesium-free PBS supplemented with 0,1% BSA (1/2 PBS) previously used. Then the cells were mixed and re-suspend with the pipette and left them to re-aggregate in agarose-coated wells. After an hour, the aggregates were completely mixed in all conditions. Finally, the cells were cultured at 14,5ºC for 24hours and then analysed. All the experiments were done in triplicate.

2.6 Preparation and graft of coated beads

For the experiment involving protein-coated beads, heparin beads (Sigma, H563) were first washed thoroughly with sterile PBS, dried and dissolved in the specific protein solution diluted in PBS. In all the protocols carried out on this thesis, the beads were incubated ON at 4ºC with the peptide/antibody solution.

To perform the beads graft *in vivo,* embryos were peeled half an hour before the beginning of the procedure. A small incision was performed in the animal cap and the beads were inserted inside the blastocoel cavity with the aid of sharp-edged forceps. Embryos were kept immobilised until the wound was healed. During the graft, embryos were kept in 3/8 NAM.

For the *in vitro* assays, a thin line of silicone grease (VWR 6366082B) was drawn over the fibronectin-coated surface of the plastic dish and DFA was added right after that. Then the beads were inserted under the silicone grease and immobilised at its border. Subsequently, Deep Layer explants were cultured in front of each bead.

Table 1 . List of proteins used for the *in vivo* and *in vitro* experiments

Peptide ID	Sequence	Working Concentration
C3adesArg[1]	H-RYYEKKREAEKLSKDDDTLG-COOH	0.7 µM
C3a[2]	H-RYYEKKREAEKLSKDDDTLGR-COOH	0.7 µM

[1,2] (Hugli, 1990).

2.7 Obtaining and stocking DNA clones

Small amounts of plasmid DNA were usually obtained either spotted on a filter paper or as a small colony of transformed bacteria. If on the filter paper, the spotted region was cut out and resuspended in water for several minutes at 37ºC. Then 2 uL were taken and added to 20 uL of competent Dh5a E.coli cells and left on ice for 45 minutes. After this, a short heat shock (50 seconds at 42ºC) was given to the bacteria tubes and then they were resuspended on 500uL of S.O.C medium (Invitrogen). The tubes were incubated for one hour at 37ºC. The tube content was then plated on LB agar plates containing an antibiotic for selection (typically ampicillin or kanamycin) and left overnight at 37ºC and the presence of colonies was expected next morning. With a sterile micropipette tip one isolated colony was picked up and grown overnight in 3mL

of LB medium with antibiotic in agitation. At the next day, the cells were pelleted by centrifugation (10 minutes, 4000rpm) and the supernatant was discarded. The plasmid DNA was isolated using the Plasmid Midi Kit (Quiagen, 12143). Concentration was measured using the NanoDrop Spectrophotometer (ND-1000) and DNA quality was estimated by running the eluted product in an agarose gel.

2.8 Enzymatic DNA restriction

Ten micrograms of plasmid DNA were digested either at the 3′ restriction site (for sense mRNA) or at the 5′site (for antisense probes) with the appropriate endonuclease. 100 uL reaction was prepared with 10µL of the appropriate 10X restriction buffer, 1µL of BSA and 1µL of the enzyme, all diluted in nuclease free water. Enzymes, buffers and supplementary BSA were purchased from Promega. The digestion was left for at least two hours at 37ºC and the reaction efficiency was assessed by running 1/100 of the reaction volume on an agarose gel.

Digested plasmids were then purified through phenol-chloroform extraction and EtOH precipitation. To do that, the original reaction volume was raised up to 200 µL with DEPC-treated water. The same volume of Phenol:Chloroform:Isoamyl alcohol (25:24:1) was added, mixed vigorously and centrifuged at 4ºC for 10 minutes at 13,000 rpm. The upper layer was then taken and added to a fresh 1,5 mL eppendorf tube. Two volumes of 100% EtOH (400 µL) and 1/10 of the total volume of Sodium Acetate were added to the tube. The solution was mixed by vortexing and incubated for no less than three hours at -20ºC to promote DNA prepititation. After that, the mix was centrifuged for 10 minutes at 13,000 rpm at 4ºC. The supernatant was removed and 350 µL of 70% EtOH added and centrifuge at 4ºC for 10 minutes at 13,000 rpm. This step ensures that no salt traces are present in the final DNA solution. After centrifugation, the supernatant was discarded and the DNA pellet was let to dry. When all the EtOH had been eliminated, DNA was diluted in 20µL of nuclease-free water.

Finally, the efficiency of the purification and precipitation was quantified by measuring the final amount of purified DNA on the NanoDrop.

2.9 Morpholino synthesis for microinjection

Antisense, Oligo-morpholinos were designed as recommended by Gene Tools or using information from published data. The following MOs were used during this project: C3MO (5'-ACTGGACAATGTGCAAACTTTGAAT-3'), C3aRMO (Carmona-Fontaine et al., 2008; Carmona-Fontaine et al., 2012) and a Standard Control MO (5'-CCTCTTACCTCAGTTACAATTTATA-3'). C3 and C3aRMO were designed against the 5-UTR C3 and C3aR gene respectively. Standard Control MO was used to assess toxicity of equimolar concentration of working MO concentration.

2.10 Synthesis of antisense RNA probes for in situ hybridization

Two µL 5′ linearised and purified plasmid DNA containing the gene of interest were mixed with the transcription mixture. In vitro transcription of antisense RNA was performed using T7, T3, or SP6 RNA polymerase (Promega) following the instructions provided by the manufacturer. The NTP-mix used for the reaction contained 0.35mM digoxigenin-labelled UTP, resulting in the production of a digoxigenin-labelled RNA. RNA was purified using the RNeasy kit (Qiagen, 74104) and the DNA traces were eliminated using the DNAse step provided by the kit. RNA concentration was measured using the NanoDrop. Probes were diluted in hybridisation buffer up to working concentrations (empirically determined).

2.11 Whole Mount in situ hybridization

In situ hybridization protocol was adapted from standard protocols (Harland, 1991). To avoid RNA degradation, all the solutions including the post-hydrization washes were prepared using DEPC-treated water.

First of all, embryos were fixed with MEMFA (see solutions section) for one hour at room temperature or overnight at 4ºC, washed with PBS for 10 minutes and kept in 100% MetOH at -20ºC. To continue with the procedure, embryos were rehydrated by successive washes with 75%, 50%, and 25% methanol. To remove the pigment of the cells, embryos were bleached in bleaching solution protected against the light during the first 15 minutes and then under the light until no sign of pigment was detected. 25% methanol catalyses the bleaching reaction, therefore, some 25% methanol was left in the tube.

After bleaching, embryos were washed with PBS for 15 minutes at RT (three washes of five minutes each) and re-fixed with MEMFA for 30 minutes at RT. After further washes with PBS, embryos were transferred to hybridization buffer and incubated at 62ºC for no less than four hours before adding the probe. The digoxigenin-labelled probe was then added and incubated with the embryos ON at 62ºC.

After hybridization, embryos were washed in a set of five solutions of decreasing SSC/Formamide percentage for 10 minutes each, except for the washing solution 5, in which embryos were incubated for 30 minutes (for more information, see 2.14). The embryos were then rinsed with Maleic Acid buffer (MAB) and blocked in 2% BMBR (Boehringer Mannheim blocking reagent; Roche) diluted in MAB for at least two hours. Embryos were incubated ON at 4ºC with anti-digoxigenin antibody conjugated with alkaline phosphatase (Roche) diluted in the same blocking solution (BMBR2% in MAB).

The next day, any excess of the antibody was removed by six consecutive washes of 30 minutes each with MAB at room temperature. Alternatively, two washes of 30 minutes can be done followed by a ON wash at 4ºC. After the washes, embryos were transferred to Alkaline Phosphatase buffer and the developing reaction was performed using 75ug/mL BCIP (5-bromo-4-chloro-3-indoyl-phosphate; Roche) and 150 ug/mL NBT (4-nitro blue tetrazolium chloride; Roche) at RT. The developing solution was removed as soon as a signal of background colour started to be observed in the embryos, thus

blocking the reaction. To remove any background staining, embryos were washed in 100% methanol for 30 minutes at RT. Finally, embryos were rehydrated by adding PBS and then fixed in MEMFA for storage at 4ºC.

To visualise the injected area, embryos were treated with Glycine solution for 30 minutes at RT, then washed in MAB, blocked for 30 minutes with BMBR 2% in MAB and incubated with an anti-fluorescein-AP antibody (Roche) at 4ºC ON. Embryos were then washed with MAB and transferred to AP buffer. To distinguish ISH staining from the fluorescein staining, BCIP alone was added to the AP solution, resulting in a light blue colour. Reaction was stopped by rinsing the embryos in PBS and background staining was removed by incubating embryos in 100% MetOH for half an hour. Finally, embryos were hydrated with PBS and fixed for storage in MEMFA at 4ºC .

2.12 Western Blots

To perform protein expression analysis, Superficial Layer and Deep Layer explants were isolated as explained in 2.4 . To get enough amount of protein, at least fifty explants were used per experiment. Explants were homogenised with approximately 100uL of homogenisation buffer containing 1/25 of phosphatase inhibitor cocktail (ThermoScientific)

Homogenised explants were incubated at 4ºC for 10 minutes, vigorously vortexed and centrifuged at 4ºC for 15 minutes at 13,000 rpm. The supernatant was then collected and placed in fresh tubes. Protein extracts were then aliquoted and kept at -80ºC for storage.

Gels with different percentage of acrylamide were prepared, according to the purpose of each experiment. 10-15% acrylamide was normally used in our experiments due to the size of the proteins analysed.

To run the gels, samples were diluted in Loading Buffer (Invitrogen, NP0007). To analyse C3a expression, samples were boiled for 5 minutes at

99ºC, however due to the fact that C3aR is a GPCR, for C3aR expression analysis, the protein solution with the correct amount of loading buffer were left for four hours at room temperature without boiling it. The electrophoresis chamber was filled with running buffer (see solutions section), the gel was assembled and the protein samples loaded. Due to the low amount of protein in our explants, 35 µL of protein solution was usually loaded to the gel. To estimate the size of the bands obtained, a protein standard ladder (Fermentas) was placed next to the protein samples. Electrophoresis was performed at 150V during 90 minutes.

When the front of the gel reaches 70% of the resolving distance, sponges and filter papers were incubated with the transfer buffer (see solution section). PVDF membrane (Amersham Hybond) was activated by incubating in 100%MetOH, washed with filtered water for one minute and incubated in transfer buffer before the assembly of the transfer sandwich.

A semi-dry blotter was used to transfer the protein from the gel to the membrane. Transfer was performed at 150V for 90 minutes. Transfer efficiency was assessed by incubation of the membrane in Ponceau Red solution for one minute. The membrane was washed with 1%Tween PBS solution to remove the Ponceau traces and blocked with 5%milk in PBS for an hour at RT. Then the membrane was incubated with the desired primary antibody diluted in 1-4%milk in PBS overnight at 4ºC. Excess of primary antibody was removed by extensive washes of the membrane with PBS. The membrane was then incubated with the secondary antibody solution for an hour at RT and washed after that to remove the excess of secondary antibody solution. To visualise the bands, the membrane was incubated with ECL (Thermoscientific) and developed using a digital developer.

2.13 Photography of fixed embryos

Embryos was immobilised in an agarose-coated dish and photographed with a Leica DFL420 camera attached to a Leica MZFLIII dissecting microscope. IM50 software (Leica) was used to capture the images.

2.14 Cell tracking and chemotaxis index (FMI) calculation

Time-lapse frames of individual deep layer cells or centre of mass of different explants were manually tacked using the Manual Tracking tool of ImageJ. This method requires a manual identification of each cell at each time point. Because usually a low magnification and relatively long distance in between frames were used in these analysis, there was no need to identifu the centroid of any specific landmark to locate the cells accurately. If tracks were performed at higher temporal and/or spacial resolution, the centroid of the cell or nuclei was determined and used for tracking. Matrices containing the x,y data of each cell at each time point were imported to Matlab were a script was written to analyse them (Carmona-Fontaine et al., 2008).

Expansion of the ectoderm for Figure 3.2f was quantified my measuring the distance of selected cell nuclei at stage 11 (d_c). The selected cells were traced back to their ancestors at stage 9 by manual tracing and the distance of the ancestor´s nuclei (d_a) was measured. Expansion for each cell pair is calculated as: $e = d_c/d_a$. The reported expansion of the cell layers is the average of all the measured cell paired expansions.

Automatic tracking of cell nuclei of *in vivo* superficial layer (Figure 3.2e) was performed using the DCU CIPA TRACKER software (Hossain et al., 2011; Thirusittmapalam et al., 2013).

To calculate the Chemotactic Index (CI), the movies were rotated to have the y-axis passing through the source of chemoattractant at the top of the cells. The CI or Forward Migration Index in the y-axis corresponds to the cosine of the angle between the displacement of the cells and the y-axis (Kay et al., 2008). The x_{FMI} and y_{FMI} represent the efficiency of the forward migration of cells, in relation to the x- or y- axis. The larger the index on an axis, the stronger the chemotactic effect is on this axis. For example, a FMI of 1 denotes that the cell

is going directly towards the chemoattractant source. For simplification, it is assumed that either the x-axis or the y-axis is parallel to the direction of the chemotactic gradient (taken from www.ibidi.com).

2.15 Embryo sectioning

Embedding

Embryos were fixed in MEMFA or 3.7% formaldehyde in PBS for one hour at room temperature. The embryos were then quickly rinsed in Phosphate Buffer and transferred to a solution of 15% sucrose in Phosphate Buffer 1X overnight at 4°C (see solutions section).

Next day, the embryos were transferred to a solution of Sucrose and Gelatine in Phosphate Buffer for at least two hours at 42°C. In the meantime, some gelatine is placed at the bottom of the mould and let it solidify at room temperature. The embryos were then placed on top of the gelatine layer. Each embryo is placed in a drop of gelatine (42°C) and the mould is filled up to the brim with gelatine solution as well. (Make sure that previously solidified gelatine is mixing with newly added gelatine).

Freezing

Before cutting the blocks out of the gelatine, 50mL of isopentane is kept at -80°C to chill it out.

Gelatin-embedded embryos were taken out using a sharp scalp and placed under a dissecting microscope to orientate the gelatine cubes according to the kind of section that was done. Once the block is correctly oriented, samples were sticked on a piece of paper using a drop of OCT compound. Cut blocks were transferred to cold isopentane for one minute at -80°C. After that, isopentane were removed and embryos kept at minus 80°C for as long as needed it.

<u>Post-cutting procedure</u>

   To remove gelatin, the slides were incubated in PBS at 37ºC for half an hour and incubated with 1/1000 DAPI and rhodamine Phalloidin for one hour at room temperature. After the incubation to remove excess of the staining dyes, sections were washed three times in PBS for five minutes each wash.Slides were mounted using 100 µL of Mowiol (see solution section) and a coverslip were placed on top of the slide. Number of cell layers was counted at 10 positions in each embryo

2.16 Mediums and buffers for embryo and animal maintenance

<u>Egg-laying medium (Ca^{2+} free)</u>

  - 110 mM NaCl

  - 2mM KCl

  - 0,6mM Na$_2$HPO$_4$

  - 15mM Tris Base

  - 2mM NaHCO$_3$

  - 0,5mM MgSO$_4$

Adjust pH to 7.6 with acetic acid

<u>10X Modified Ringer Solution (MMR)</u>

- 1M NaCl

- 20mM KCl

- 10mM MgSO$_4$

- 20mM CaCl$_2$

- 50mM HEPES

- 1mM Disodium-EDTA

Adjust pH to 7.6

<u>Normal Amphibian Medium</u>

- 1.1M NaCl

- 20mM KCl

- 10mM $Ca(NO_3)_2$

- 10mM $MgSO_4$

- 1mM Disodium-EDTA

Normal Amphibian Medium B

- 20mM NaH_2PO_4

Adjust pH to 7.5

Normal Amphibian Medium C

- 100mM $NaHCO_3$

Working Concentration for 1L NAM

	NAM A	**NAM B**	**NAM C**	**water**
1/10 NAM	10 mL	10 mL	1 mL	979 mL
3/8 NAM	37 mL	37 mL	1 mL	925 mL
3/4 NAM	74 mL	74 mL	1 mL	851 mL

Add 1mL of Streptomycin (50g/L)

Tricane Solution

5g of Ethyl 3-aminobenzoate methanesulfonate

Add H_2O up to 1L

Ficoll (solution used to inject embyos)

3% Polysucrose in NAM3/8

DFA solution

- NaCl 53mM

- Na_2CO_3 5 mM

- K-Gluconate 4.5mM

- Na-Gluconate 32mM

- $MgSO_4$ 1mM

- $CaCl_2$ 1mM

- BSA 0.1%

Adjust pH to 8,3. Add Streptomycin 50 ug/mL

2.17 Solutions for the in situ hybridization protocol

<u>MEM 10X solution</u>

- MOPS 1M

- MgSO$_4$ 10mM

- EGTA 20mM

In DEPC-water

<u>MEMFA (1mL)</u>

- 8 mL of DEPC-treated water

- 1 mL 10X MEM

- 1 mL of Formaldehyde

<u>SSC20X</u>

- NaCl 3M

- Tri-sodium citrate 0.3M

Adjust pH to 7.0

<u>Bleaching solution</u>

- H$_2$O$_2$ 20%

- Formamide 5%

- 20x SSC 2.5%

in DEPC-water

<u>Hybridisation Buffer</u>

- Formamide 50%

- SSC 5x

- Denhardt's Solution 1X

- Ribonucleic acid 1mg/ml

- Heparin 100µg/ml

- CHAPS 0.1%

- EDTA 10mM

- Tween-20 0.1%

Adjust pH to 5.5

Labeled NTP-mix (10x)

- 10mM GTP

- 10mM ATP

- 10mM CTP

- 6.5mM UTP

- 3.5mM Dig/Fluo-UTP

Solutions for post hybridisation washes

	Formamide	**SSC20X**
Solution 1	50 mL	10 mL
Solution 2	25 mL	10 mL
Solution 3	-	10 mL
Solution 4	-	10 mL
Solution 5	-	1 mL

DEPC-water up to 100 mL

Maleic Acid Buffer

- Maleic acid 100mM

- NaCl 150mM

2.18 Western Blot solution

Protein Buffer (PB)

Tris   3,027g (250mM)

Glicine 144,2 g (1921mM)

Adjust pH to 8.3

Running Buffer (1X)

- Protein Buffer (to 1x)   10%

- SDS 0.1%p/v

Transfer Buffer (1X)

- Protein Buffer (to 1x) 10%

- Methanol 20%

- SDS (Optional) < 0.1%p/v (usually 0.03%)

2.19 Solutions for sectioning

Phosphate Buffer (PB). Stock Solution 2X

- NaH_2PO_4 3.2g

- Na_2HPO4 13.5g

For 500 mL

Sucrose 15% in PB 1X

- In a 50mL tube put 25mL of 2X PB, add 7,5g of sucrose, then fill up to 50mL
  with distilled water. Vortex to dissolve.

Gelatin 7,5%-Sucrose 15% in PB1X

- In a 50mL tube put 25mL of 2X PB, 7,5g of sucrose. Dissolve the sucrose
before adding the 3,75g of gelatin on top. Heat the tubes at 42ºC is required for
completely dissolve the gelatin (usually, no less than four hours). Once is
dissolved, fill up to 50mL with distilled water*.*

Part III: Results

3.1 C3a/C3aR is expressed in the ectoderm during gastrulation

Scanning electron microscopy shows the topography of embryos before gastrulation (stage 9), at the onset of gastrulation (stage 10) and after gastrulation had already started (stage 11) (Figure 3.1a). In the resulting images, cells from the superficial layer were coloured in red and intermediate and most deep cells were coloured in light and dark green respectively (Figure 3.1a). Before the beginning of gastrulation, at stage 9, the ectoderm of *Xenopus* embryos consists on a three-layered epithelium with an outermost superficial layer of cells (red cell layer in Figure 3.1a); and two layers of underlying deeper cells (light and dark green cell layers in Figure 3.1a). As development progresses (S10 and S11), the deep layer cells rearrange into a single layer by interdigitation of deep cells along the animal cap (compare light and dark green cells in S9 with S11 on Figure 3.1a). Although no differences in number of cell layers were found between stage 9 and 10 (green cells in S9 and S10 in Figure 3.1a) deep cells from stage 10 embryos showed a distinct shape with higher number of protrusions (light and dark green cells in S9 and S10), while the superficial layer showed a very epithelial-like compact shape (red cells in S11). Thus, we decided to focus on stage 10 ectoderm, for it is the stage where superficial and deep cells can be relatively easily discriminated. Furthermore, at this stage deep layer cells display a motile feature and finally, it is the onset of gastrulation.

With the aim of finding novel molecules that could be involved in the regulation of cell behaviour in the animal cap, we decided to explore the expression of complement genes at stage 10. We then performed *in situ* RNA hybridization (ISH) for a group of complement factors: C7, Properdin, CFH and C3. Intriguingly, we observed that Complement C3, a potent chemoattractant shows a strong, punctuate pattern in the ectoderm, with higher expression in the dorsal than in the ventral side of the animal cap (Figure 3.1b). ISH using the sense C3a mRNA did not show any staining (data not shown). Levels of expression in the ventral and dorsal regions were quantified and compared with the expression level in the whole animal cap, showing an approximate 50%

reduction in the ventral region and an approximate 50% increase in the dorsal region when compared to the averaged animal cap. Interestingly, expansion in dorsal regions is significantly higher than in ventral regions (data not shown). This asymmetry might contribute to known dorso-ventral differences in gastrulation of *Xenopus* embryos (Bauer et al., 1994). The presence of C3 so early in development is also intriguing as no immune system, blood or circulation is yet established in these embryos.

We then performed sagittal sections of the whole embryos after ISH against C3 and sections were counterstained with DAPI (Figure 3.1d and e) Interestingly, we found that while C3 mRNA was expressed in the most superficial cells of the animal cap, it was undetectable in the deep cells (zoomed section in Figure 3.1e). Furthermore, to identify which cell type within the animal cap expresses C3 and its receptor at the protein level, we performed protein analysis by Western Blot against C3a and its receptor C3aR (figure 3.1f) on the superficial layer and deep layer explants shaved from the dorsal animal cap (summarising drawing in Figure 3.1f). Consistent with what we observed for the mRNA, western blot confirmed that C3a and C3aR have distinct expression patterns: C3a is expressed in the superficial layer while C3aR is mainly expressed in the deep layer. C3a and C3aR antibody specificity had already been tested in previous studies (Carmona-Fontaine et al., 2008; Carmona-Fontaine et al., 2012; unpublished data).

These results, together with the fact that C3a acts as a strong chemoattractant, led us to speculate that the C3a produced by the superficial layer could regulate the chemotactic movement of deep layer cells at the onset of gastrulation.
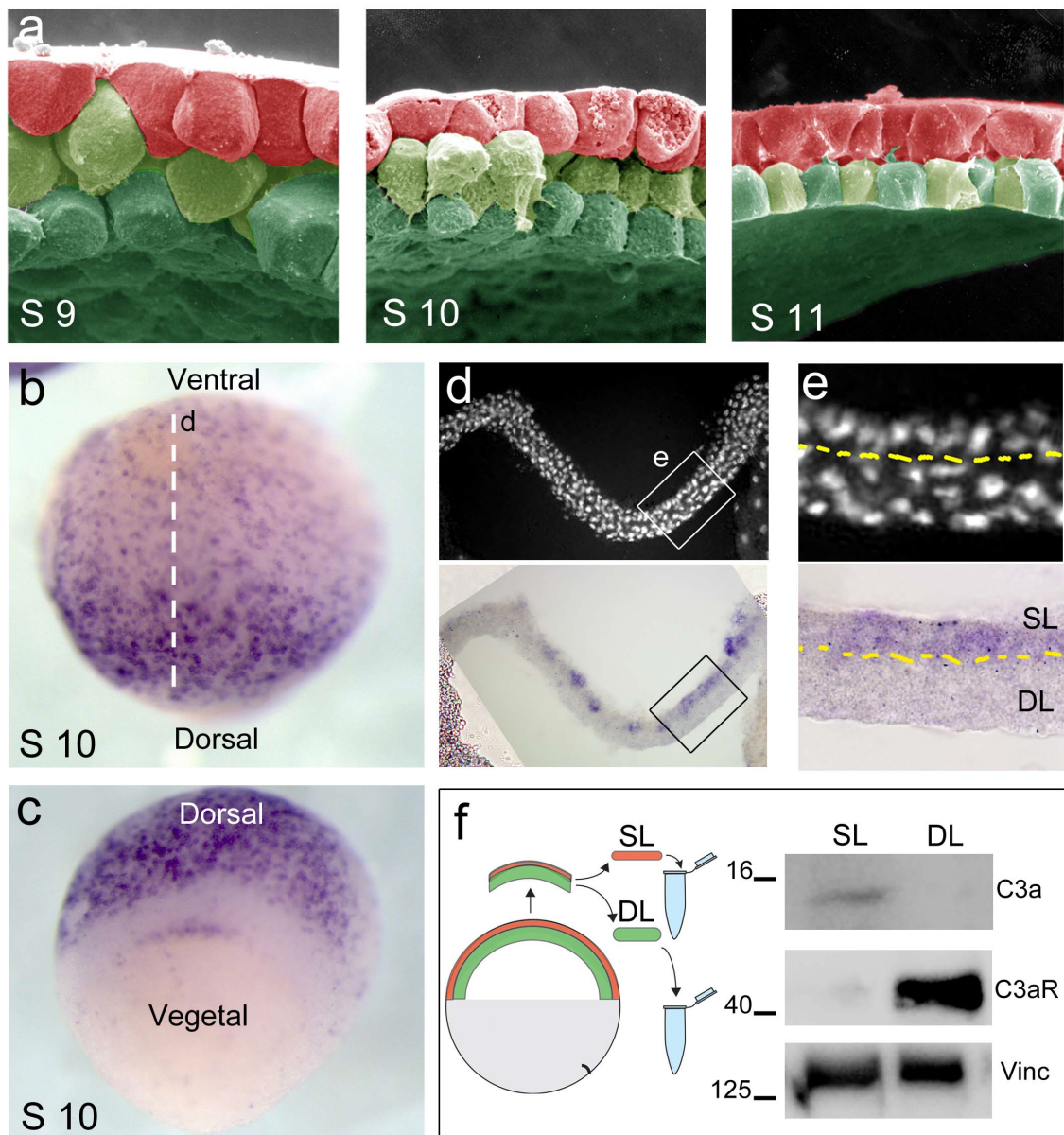
Figure 3.1. C3/C3aR are expressed in the ectoderm during gastrulation. (a) SEM of ectoderm during gastrulation at the indicated stages. Superficial cells are false coloured in red and deep cells in two shades of green. Note the thinning of the ectoderm from stage 9 to stage 11. (b, c) C3 in situ hybridization at stage 10, in animal (b) and dorso-vegetal (c) views; d: indicate section. (d) Section of embryo shown in b; upper panel: DAPI staining; lower panel: C3 in situ hybridization. (e) Zoom of section shown in d. Note that C3 is expressed only in superficial (SL) and not in deep (DL) layer. (f) Western blot against C3a and C3R for the superficial (SL) and deep (DL) layers. Vinc: vinculin is used as loading control. Figures in Panel a were kindly generated by Rey Keller.

3.2 C3 is required for epiboly during gastrulation

During gastrulation, the blastocoel roof becomes thinner as epiboly proceeds in a process that requires local cell movement (Keller 1978; Keller 1980). This prompted us to analyse whether the inhibition of C3aR through morpholino (MO from here on) interference would have an impact in epiboly and thinning of the ectoderm during *Xenopus* gastrulation.

In order to address this, we injected either CoMO or C3aRMO in the four animal blastomeres of eight cell-stage embryos. Embryos were fixed at stage 11 and sagittal sections of the whole embryos were counterstained with DAPI to quantify the number of cell layers. A total of 20 embryos were analysed for each conditions. For the whole thesis, experiments shown were performed with embryos from at least three different fertilisation where the females had been taken randomised from independent water tanks.

Blockage of C3aR expression inhibited the thinning of the ectoderm as shown by the highly significant increase in the average number of cell layers, which changed from two in the CoMO-injected embryos to five in C3aRMO injected ones (Figure 3.2a and b). As expected, the thickness of the ectoderm was also increased in the C3aRMO-injected embryos when compared to the CoMO-injected controls, from 20 μM to almost 40 μM of thickness (Figure 3.2c). These results imply that C3aR is required for proper ectodermal epiboly and thinning during *Xenopus* gastrulation.

In order to test whether the defects in epiboly would be regulated by an abnormal cell movement in the ectoderm, we performed time-lapse movies of the superficial ectodermal cells of embryos co-injected with a mixture of fluorescent nuclear and membrane markers, and either CoMO or C3aRMO. Embryos were injected in the four animal blastomeres of an eight cells-stage embryo. Embryos were filmed from stage 9 (time 0) until sibling control embryos reached stage 11 (time 240 min). Individual cells were tracked throughout the course of the movie using the FiJI Manual Tracking (Figure 3.2d) tool (see

section 2.14). Upon C3aR depletion, cells of the superficial ectoderm displayed decreased motility as can be observed from the change in the movements profile displayed in Figure 3.2e and from the reduced walked distance by C3aRMO-injected cells when compared to the control (Figure 3.2f). Altogether, these results suggest that C3aR is required for the movement of superficial ectodermal cells during gastrulation.

We then decided to further explore the contribution of C3aR to the regulation of the superficial cells movement. As the superficial layer expands during epiboly, we tested whether C3aR depletion in the ectoderm would also reduce the expansion of the ectoderm during epiboly. The same movies used in Figure 3.2e-f were used to calculate expansion of the ectoderm from stage 9 to stage 11. (Expansion of the ectoderm was calculated dividing the distance between two cells cells at stage 11 by the distance between the same two cells at stage 9). Interestingly, upon C3aR depletion, the expansion of the ectoderm was reduced, as shown by the significant reduction on the expansion index (Figure 2g). This result suggests that C3aR is required for the expansion of the superficial layer of the ectoderm during epiboly.
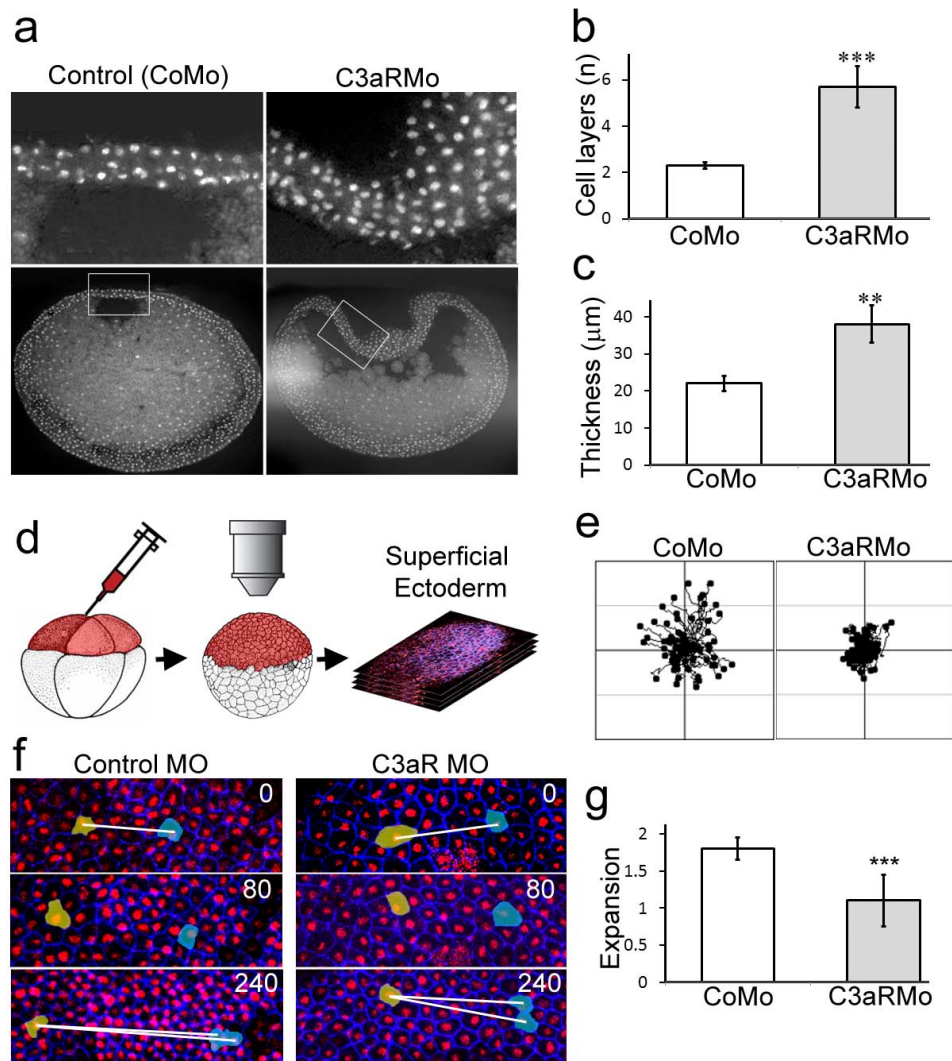
Figure 3.2. C3 is required for epiboly during gastrulation. (a) Sections of stage 11 embryos injected with control MO or C3aR MO and stained with DAPI. Note the two cell layer in control embryos, whereas there are many more cells layers in C3aR MO embryos. (b) Number of cell layers at stage 11. (c) Thickness of the ectoderm at stage 11. (d) Embryos were injected with fluorescent nuclear and membrane markers together with control MO and C3aR MO and analysed by time lapse imagining from stage 9 to stage 11. Only the superficial ectoderm is visible. (e) Tracks of control and C3aR MO ectodermal cells during gastrulation. Note the reduced cell movement in C3aR Mo embryos. (f) Frames of time lapse moves at the indicated times and treatments. Pair of single superficial cells were followed and their distance was recorded at stag 9 (0h) and at stage 11 (24h). (g) Expansion of ectoderm was calculated by dividing the distance between pair of cells at stage 11 by the distance between the same pair of cell at stage 9. Note the reduced expansion in C3aR MO embryos. Panels d-g were generated by Shariff Omar and Andras Szabo.

3.3 C3aR does not affect cell adhesion during gastrulation

It has been suggested that during *Xenopus* gastrulation, adhesion to fibronectin (Marsden and De Simone, 2001; Longo et al., 2004) is essential for epiboly of the ectoderm. Also, in zebrafish, cell adhesion of deep cells with each other and with the superficial cells is required for proper epiboly (Babb and Marrs 2004; Kane et al., 2005; Shimizu et al., 2005; reviewed in Lepage and Bruce 2010). Therefore, we tested whether inhibition of C3aR in the ectoderm affects any of the adhesion parameters.

In order to test a possible role of C3aR in cell-cell adhesion, two experimental approaches were used. First, deep ectoderm cells were taken from embryos and injected with a combination of either CoMO+FDX (green) or C3aRMO+RDX (red). (Figure 3.3a). The cells from each group of embryos were dissociated using low calcium media, mixed and deposited on a layer of fibronectin (Figure 3.3b), superficial cells (Figure 3.3c) or deep cells (Figure 3.3d). Two hours later, the dishes were flipped over, the non-attached cells were discarded and the remaining attached cells were counted (see section 2.5). Pictures were taken immediately after cell seeding (0h) and after flipping the dish (2h). Interestingly, no different adhesion towards fibronectin, superficial or deep cells was observed between CoMO and C3aRMO cells (frames below the drawing in Figure 3.3a, b and c and statistical analysis for three independent experiments is shown in Figure 3.3f). As a positive control, deep layer cells injected with E-cadMO were used in this experiment. As expected, a significant proportion of cells injected with Cdh1 morpholino detached from the monolayer, when compared to the CoMO injected cells (red and green cells in Figure 3.3e respectively).

In a second experiment we performed a cell-sorting analysis in which deep ectodermal cells injected with either CoMO+FDX or C3aRMO+RDX were dissociated, mixed and cultured on agarose for 2h (drawing in Figure 3.3g). The sorting experiment showed no different between CoMO-injected cells (red and green cells in Figure 3.3h) nor between CoMO-injected deep cells and C3aRMO-injected deep cells (red and green respectively in Figure 3.3i). As a positive control, deep layer cells injected with CoMO (red) were mixed with

Cdh1 morphant deep cells, showing the expected cell-sorting behaviour (Figure 3.3j). These results suggest that even though we cannot completely rule out that C3aR have minor, undetectable effects on cell adhesion, it is unlikely that it can explain the strong effect in epiboly and cell motility of the ectoderm cells observed in embryos where C3aR has been depleted.
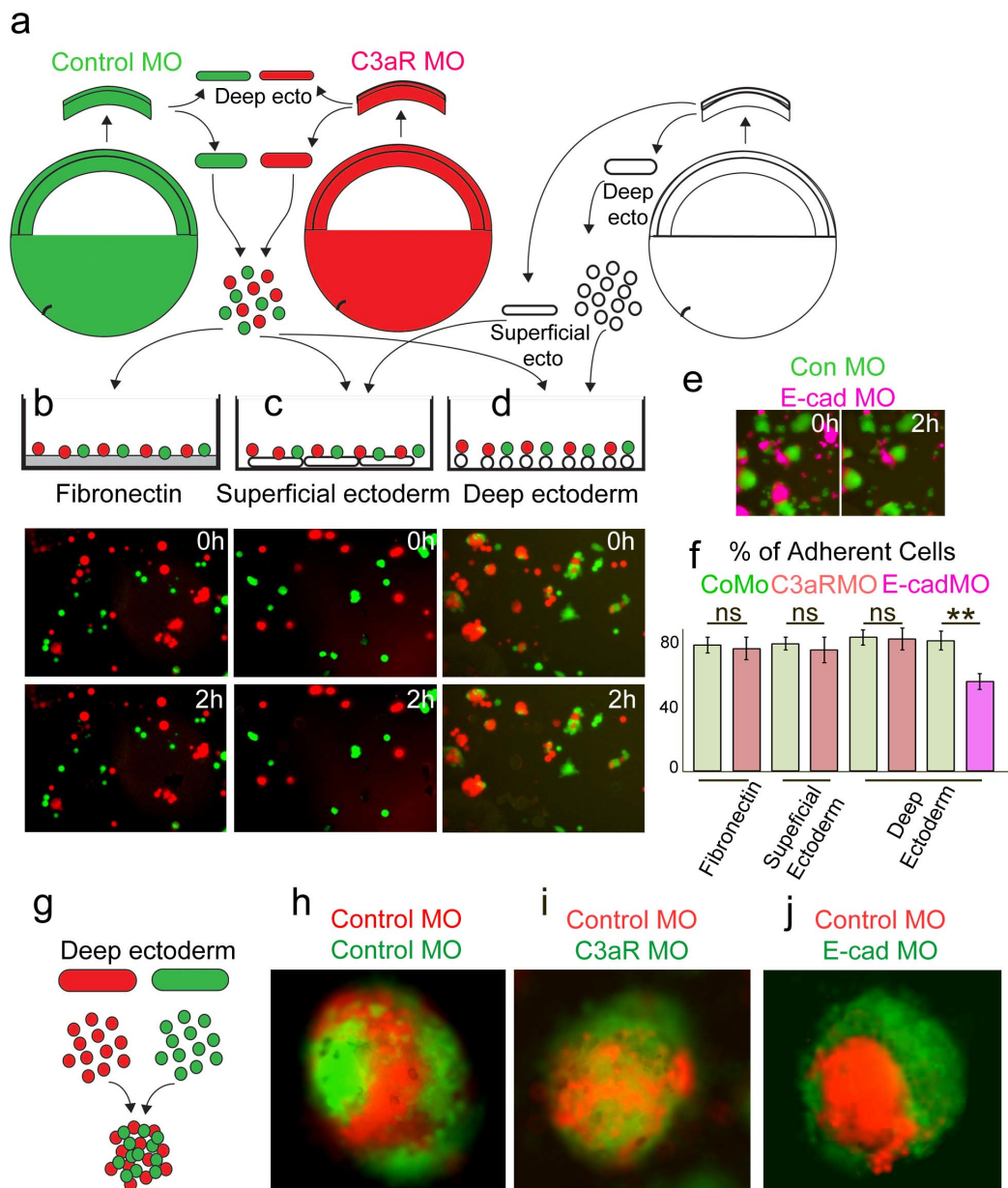
Figure 3.3. C3 does not affect cell adhesion during gastrulation. (a) Deep ectoderm cells taken from control MO (green) or C3aR MO (red) cells were dissociated, mixed and cultured on fibronectin (b), on a layer of superficial cells (c) or on a layer of deep cells (d). After two hours the dishes were flipped over and non-attached cells were removed. Pictures were compared immediately after cell culture (0h) and after filliping the dish over (2h). As control deep cells were taken from embryos injected with Cdh1 MO (e). Examples of picture at 0 and 2 h are shown and the summary of three independent experiments is shown in f. No different adhesion towards fibronectin, superficial or deep cells was observed between control and C3aR MO cells. The only reduced adhesion was observed with Cdh1 MO cells. (g) Deep ectodermal cells were dissociated mixed and cultured on agarose for 24 h to analyse cells sorting. No cell sorting was observed between Control MO or C3aR MO cells (h, i). A clear cell sorting is shown between control and cadherin depleted cells. Experiments and plots in this figure have been generously generated by Sophie McLalin and Shariff Omar.

3.4 Chemotaxis between superficial and deep cells is C3a/C3aR dependent

The absence of adhesion changes in C3aRMO depleted ectodermal cells prompted us to explore an alternative explanation to the effect that we observed following C3aR inhibition. As pointed before, the distinct expression pattern of C3a and C3aR suggested that, during gastrulation, C3a might control the movement of deep layer cells towards the superficial layer in cells undergoing epiboly. Therefore, we hypothesised that the deep layer cells would chemotactically move towards the superficial layer and that the movement would be triggered by the C3a secreted by the superficial layer.

In order to address this, we firstly decided to investigate whether the deep layer cells actually move toward the cells of the superficial layer. Animal caps from stage 10 embryos (injected with FDX or RDX to discriminate between the different layers) were dissected (Figure 3.4A) and plated, either alone or together, at a distance equivalent to one body explant. Then, the explants were filmed for $\geq$ 6h. At least 10 explants per condition were analysed.

While control explants of superficial layer or deep layer plated alone displayed a random movement (Figure 3.4a and b), deep layer cells exhibited a highly directional movement towards the superficial layer when both cell types were plated in proximity (Figure 3.4c). We also observed that deep layer cells did not move individually but as a collective group (data not shown). These results demonstrate that deep layer cells move collectively toward the superficial layer, supporting the hypothesis that chemotaxis of the deep layer cells towards the superficial layer might occur during *Xenopus* gastrulation.

We then decided to check whether C3a-C3aR axis is required for the deep layer cells to move toward the superficial layer. To address this, we performed loss-of-function experiment for both C3 on the superficial layer and C3aR on the deep layer followed by time-lapse movies analysis, as we did for the previous experiments. Embryos were injected with either control-morpholino (CoMO+FDX), C3-morpholino (C3MO+RDX), or C3aR-morpholino (C3aRMO

+FDX) at the eight-cells stage, and the superficial and deep layer were shaved from the stage 10 animal cap as described above (Figure 3.1).

Injection of CoMO in both superficial layer and deep layer cells of the ectoderm did not prevent deep cells to move towards the superficial layer (Figure 3.4c). On the contrary, the injection of an antisense C3-morpholino in the superficial (Figure 3.3d), or C3aR-morpholino (Figure 3.3e) in the deep layer, prevented the cells of the deep layer to move towards the superficial layer. The Forward Migration Index (FMI) of the deep cells was quantified, and observed that it was significantly reduced upon C3 or C3aR depletion in superficial and deep layer respectively (bar plot in Figure 3.4C).

In order to determine whether C3a can trigger deep cells movement, we performed *in vitro* chemotaxis assays using beads coated with either C3a peptide or C3adesARG (a C3a peptide that cannot bind C3aR) (Figure 3.4B). Deep layer explants from stage 10 animal caps were plated at a distance of one body explant from beads coated with either C3a or C3adesARG peptide and the explants were time-lapse filmed overnight. While deep layer cells showed no chemotactic movement towards the C3adesARG-coated beads (Figure 3.4f), the C3a-coated beads displayed a strong chemotactic attraction for the deep cells (Figure 3.4f). FMI analysis demonstrated a very significant increase in the chemotaxis index of the deep layer explants when plated in C3a-coated beads, compared with C3adesARG-coated beads (bar plots in 3.4C).

The expression of different mesodermal and ectodermal markers was not affected after C3aR MO injection (Fig 3.5), indicating that the C3a/C3aR axis does not affect ectodermal or mesodermal specification.

From these results we then concluded that C3a is sufficient to promote chemotaxis of the deep cells. Moreover, our results suggest that the movement of deep cells toward the superficial layer requires C3 expression in the superficial layer and C3aR expression in the deep layer. Our experiments also support an alternative chemotactic-mediated mechanism to explain the effect of C3aR in the ectoderm of *Xenopus* gastrulae.
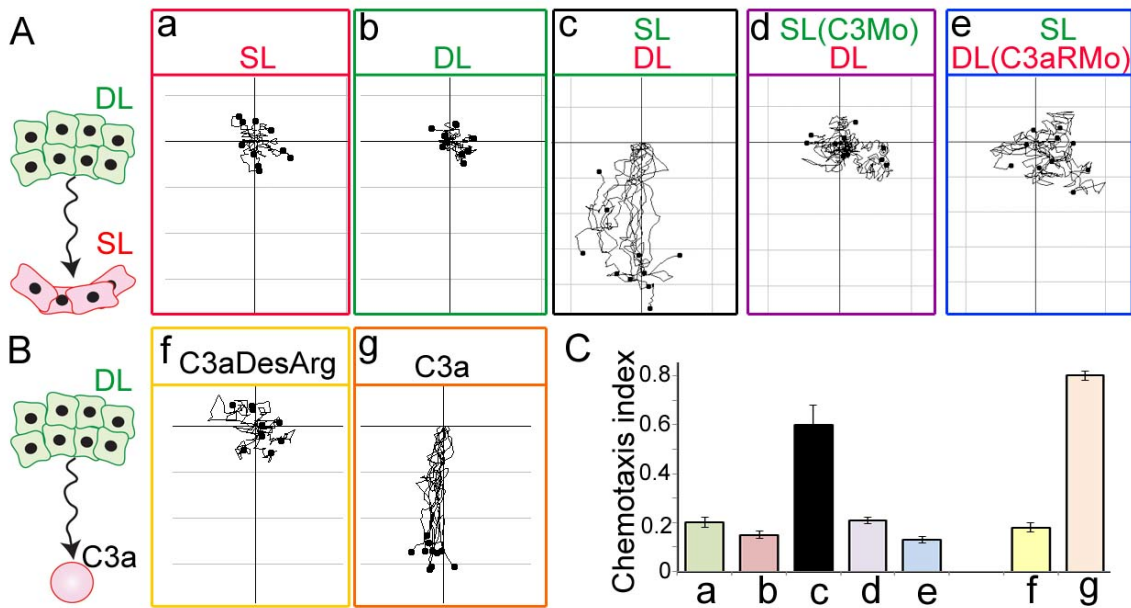
Figure 3.4. Chemotaxis between superficial and deep cells is C3a/C3aR dependent. (A) Superficial (SL) and deep (DL) ectodermal cells were dissected from stage 10 embryos and cultured at short distance, followed by time lapse microscopy, and cell tracking analysis. SL (a) or DL (b) cultured alone does not show any directional migration. (c) DL cultured next, but not in contact, to SL shows a persistent migration towards the DL. DL and SL are injected with control MO. (d) DL cultured next to a SL expressing C3 MO shows no directional migration. DL expresses control MO. (e) DL expressing a C3aR MO cultured next to SL expressing a control MO shows no directional migration. (B) Chemotaxis assay. DL was cultured next to a bead soaked with chemoattractants. Time lapse and track analysis of migrating cells was performed. (f) If C3aDesArg is used as chemoattractant no directional migration is observed. (g) If C3a is used as a chemoattractant as strong chemotaxis is observed. (C) Chemotaxis index for all the conditions described above.

3.5 C3aR is not required for ectodermal or mesodermal specification

Finally, we investigated whether the dramatic inhibition of epiboly could be explained by a failure to properly specify the germ layers during gastrulation. Therefore we examined the expression of ectoderm and mesoderm markers in C3aR morphants embryos during gastrula stages. For this, embryos were injected in the four animal blastomeres at the eight-cells stage embryos with either CoMO or C3aRMO. Similar results were obtained when embryos are injected in the equatorial blastomeres at the eight cells-stage (data not shown) Expression of ectoderm and mesoderm markers were analysed by *in situ* hybridization.

In Control Morpholino injected embryos (left column in 3.5), *keratin* is expressed in a wide region of the animal cap that will eventually form the non-neural ectoderm. This expression is not altered by injection of C3aRMO (right column in Figure 3.5). At early gastrula stages, the pan-mesodermal marker *Xbra* is expressed around the blastopore region in cells destined to become mesoderm cells. The same expression pattern was observed in C3aRMO injected embryos (Xbra in situ in Figure 3.5). No difference in body axis formation was neither observed in C3aRMO injected embryos (data not shown). At the onset of gastrulation, *Crescent* is expressed in the dorsal blastopore lip and also in a region corresponding to the dorsal marginal zone (Crescent in situ in Figure 3.5). As it happened for *keratin* and *Xbra, Crescent* expression in C3aRMO injected embryos were indistinguishable from those injected with CoMO (Crescent ISH in Figure 3.5). During gastrula stages, *Wnt8* is expressed in the ventral marginal region of the embryo (Wnt8 ISH in Figure3.5). No differences in Wnt8 expression were observed between CoMO and C3aRMO injected embryos (CoMO and C3aRMO in Wnt8 ISH, Figure 3.5)

Therefore, we could find no evidence that C3aR depletion in the ectoderm or mesoderm is involved in the initial specification of the germ layers . Instead, we can conclude that epiboly defects in C3aR morphants observed during gastrula stages is not due to an abnormal specification of the germ layer
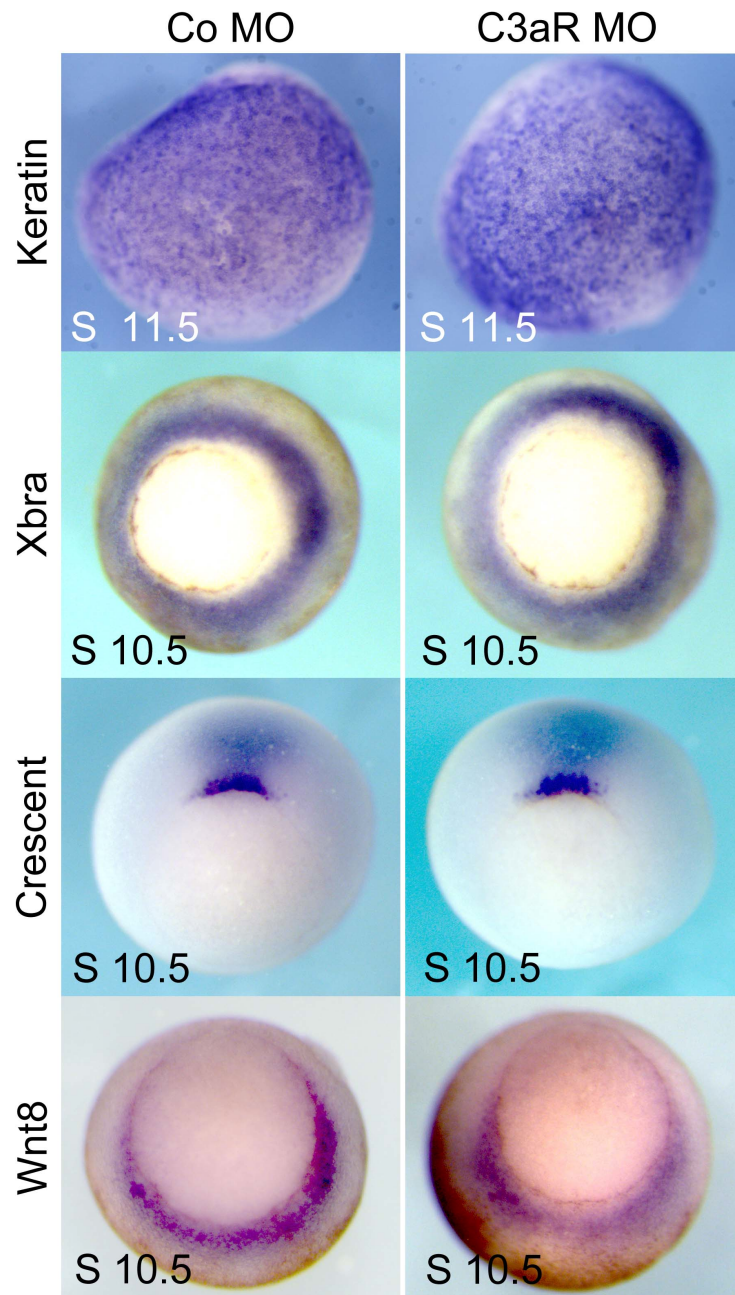
Figure 3.5. C3aR depletion does not compromise ectoderm or mesodermal specification. Eight cell-stage embryos were injected with either CoMO or C3aRMO in the four animal blastomeres. ISH against the ectodermal marker *keratin,* the pan-mesodermal marker *Xbra,* the dorsal mesodermal marker *Crescent* and the ventral mesodermal marker *Wnt8* was performed as described before. Expression in C3aRMO (right column) injected embryos was indistinguishable from those injected with standard CoMO (left column).

Summary

The aim of this project was to elucidate how complement-mediated cell interaction acts during *Xenopus* gastrulation. We observed that C3 is expressed at the onset of gastrulation in a very superficial area of the ectoderm (Figure 3.1). Interestingly, when the two cells types composing the ectoderm were analysed, we observed that the smallest C3 proteolytic fragment, C3a, was present in the Superficial Layer whereas its receptor was expressed in the most deep cell layer (Figure 3.1). During gastrulation, the ectoderm undergoes a dramatic thinning process that involves radial intercalation of deep cells. Furthermore, some reports have demonstrated that aberrant cell behaviour in the animal cap impairs gastrulation and inhibits Blastocoel Roof thinning (Marsden et al., 2001). All of this prompted us to investigate the potential role of C3a in regulating cell behaviour during epiboly. We demonstrate that C3aR is required for epiboly of the ectoderm, and that C3aR depletion in superficial ectoderm decreases cell motility and increases the expansion of the ectoderm (Figure 3.2)

Our cell adhesion experiments rules out a major contribution of cell adhesion to the effect observed in embryos whose C3aR levels have been depleted in ectodermal cells (Figure 3.3) suggesting an alternative explanation for C3aR-mediated cell behaviour.

The *in vitro* experiments showed that the Deep Layer cells move as a collective group towards the Superficial Layer (Figure 3.4). Thus, one would intuitively think that there must be some chemotactic clue coming from the Superficial Layer that promotes deep layer movement. We know that C3a is a potent chemotactic molecule with a crucial role in regulating migration of inflammatory cells and NC migration and that it is expressed only in the Superficial Layer of the ectoderm. Therefore, we explored whether C3a/C3aR (Hartmann et al., 1997; Nilson,1996; partially reviewed in Ricklin et al., 2010) signaling is indispensable for Deep Layer movement towards Superficial Layer. By using specific antisense MO against C3 and C3aR, we demonstrated that

C3aR expression in the deep layer cells is crucial for their movement towards Superficial Layer. We also showed that C3a is sufficient to promote directional migration of Deep Layer explants *in vitro* (Figure 3.4). Altogether, our results

strongly suggest that C3a is the chemotactic molecule secreted from the Superficial Layer that, through C3aR signalling, promotes movement of Deep Layer cells. We also demonstrate that embryos where C3a/C3aR was blocked in the animal cap show a thicker Blastocoel Roof

In summary, in thesis we show that a complement cytokine coming from the superficial layer of the ectoderm controls chemotaxis of the Deep Layer cells through C3aR towards the superficial layer, and that chemotaxis in the ectoderm is crucial for proper epiboly during gastrulation.

Part IV: Discussion

During gastrulation, the ectoderm suffers a dramatic change in thickness through epiboly, that includes radial intercalation of deep cells (Keller 1978; Keller 1980; Keller 1990), however, unlike the mesoderm, little is known about what regulates epiboly of the ectoderm. In this thesis we studied the role of ectodermal cells during *Xenopus* gastrulation and the relationship with the early expression of the complement components C3a and C3aR. Here we show that the complement component C3a and its receptor C3aR are expressed in the superficial and deep layer of the ectoderm respectively. We also describe that C3aR is required for proper chemotaxis of the deep layer of the ectoderm toward the superficial layer, thereby controlling epiboly and blastopore closure during *Xenopus* gastrulation.

In *Xenopus*, during epiboly, the deep cells of the ectoderm undergo a local migratory movement, thereby transforming several layers of cells into one single layer of greater area (Keller, 1978). Few chemokine ligands and receptors have been characterised during early *Xenopus* embryogenesis (Fukui et al., 2007; Goto et al., 2010). C3 was reported to be expressed at early gastrula stages (McLin et al., 2008). However, in this study we have expanded this knowledge and demonstrated that it is exclusively detected at the most superficial layer of the ectoderm at the onset of gastrulation. It is known that C3a, through C3aR regulates cell movement during NC migration (Carmona-Fontaine et al., 2011). This, together with the unique expression pattern of C3a and C3aR prompted us to investigate the potential contribution of these molecules in controlling cell movement in the blastocoel roof. We found that C3a secreted from the superficial layer of the ectoderm triggers the movement of deep layer cells through the expression of C3aR, thereby controlling epiboly and blastopore closure. The same increase in ectoderm thickness and delayed blastopore closure is observed in which C3MO is injected in ectoderm cells. This phenotype can be rescued by co-injection with C3a mRNA (data not shown) supporting our hypothesis that C3a (but not C3b) through C3aR regulates blastocoel roof behaviour, thickness and epiboly. This is a completely novel piece of data, which opens new questions about the role of inflammatory chemokines in regulating chemotaxis of the ectodermal cells during gastrulation.

However, in order to generate a mechanistic model linking a local cell movement (C3a-driven chemotaxis for the deep layer cells toward the superficial layer) with the generation of mechanical forces to carry out the increase in area produced during epiboly, it is important to know whether the cell behaviour is an intrinsic property of the cells that generate the force or if it is a passive response due to forces generated somewhere in the embryo. No formal proof that the deep layer cells suffer a potential stretching force from the superficial layer, or the opposite, that the expansion of the superficial layer during gastrulation is due to the movement of the underlying deep layer cells, has been provided nonetheless.

If the active model of expansion is assumed, it is unlikely that this is due to active expansion of the superficial layer over the cells of the deep layer (Keller 1980). When the superficial epithelium is cut, the wound margin gaps open, indicating that it is under tension (Keller, 1980). In the active model, if the superficial layer of the *Xenopus* gastrulae is under tension, the force for spreading must arise in the deep region itself (probably through the active radial intercalation of deep cells and subsequent shortening of deep cells). The chemotactic movement of the deep cells towards the superficial layer would then fit with this model in the way that cells from the deep layer are attracted towards the superficial layer. This movement would promote radial intercalation thereby generating sufficient force to spread the superficial layer through the movement of the underlying deep cells. Indeed, our experimental data have already answered what happens to the superficial layer when epiboly of the deep cells is blocked. If the force to expand the superficial layer comes from the deep cells as they undergo epiboly then one would intuitively think that by blocking epiboly, the expansion of the animal cap would also be blocked; this is the case for C3aRMO injected embryos (Figure 3.2). However, if deep cells chemotax towards superficial cells *in vivo,* that behaviour would generate more cell protrusions on the sides of the deep cells facing the superficial layer. Whether the deep layer show protrusive capacity towards the superficial layer remains still unknown nonetheless. Protrusion direction of deep cells measured in scanning electron microscopy images of fixed and fractured *Xenopus* embryos during gastrulation would help us to understand whether there is a strong bias towards the superficial layer or not. The presence of protrusions

towards the superficial layer would strongly suggest that chemotaxis is present *in vivo* in the blastocoel roof. Similar PDGF-A driven chemotaxis has been demonstrated during radial intercalation of deep mesoderm in *Xenopus* (Damm et al., 2011)*.*

An intriguing possibility is the harbouring of intercalation programmes on diseases in organisms during adult stages. For example, the protrusive activity of intercalating cells could bear similarities to the behaviour found in metastatic cells derived from high aggressive tumours. It could be possible that some of the "signal-sets" that are tightly regulated during normal cell intercalation are ectopically and uncontrollably expressed in tumour cells (Huang et al., 2012). However, in other contexts, intercalation switch has been shown to alleviate the progression of some diseases, as in kidney cysts (Lienkamp et al., 2012; Nishio et al., 2010).

Our proposed chemotaxis mechanism, in accordance with previous studies (Marsden and DeSimone, 2001; Petridou et al., 2013) predicts tissue-autonomous deep layer intercalation. Tissue-autonomy could be tested using a modified blastocoel roof explant (Marsden et al., 2001; Petridou et al., 2013). Briefly, mosaic-labelled deep layer tissue would be cultured beneath an unlabelled superficial layer. Membrane protrusion activity (ruffling) would be analysed in CoMO *versus* C3aRMO injected embryos. On a second set of experiments, the same time-lapse movies would be useful to analyse the deep cells intercalation in cells either appearing or disappearing at the top of the deep cell layer. According to our model, one would predict that intercalation in CoMO explants would be expected to be higher than in C3/C3aRMO injected embryos. Finally, the modified BCR experiment would also be helpful to analyse whether the movement of the deep cells is mono-directional (towards the superficial layer only) or bi-directional as it happens in *zebrafish* (Bensch et al., 2013) with cells going towards the superficial layer and downwards to other deep cells. Bi-directional movement of deep cells seems counterintuitive in the context of our chemotaxis model. Even when the deep cells would be compelled to move actively towards the superficial layer by chemotaxis, volume exclusion could physically cause cells to move passively away from the superficial layer. However, even though we have demonstrated that deep layer

explants chemotax towards the superficial layer, whether individual cells do actually chemotax in the same way as the cell cluster remains still unknown. If chemotaxis is playing a role in regulating radial intercalation *in vivo* this is very likely to partake at the level of individual cells (Keller, 1980). To address this point, the same experiment shown in Figure 3.3. could be done using dissociated deep cells. Also, one would ask what does it happen in individual cells within deep layer explants when they are exposed to a source of C3a (superficial layer or C3a-coated beads). Do the cells undergo radial intercalation with other deep cells upon migrating towards the C3a source? Mosaic knock - down of C3aR in deep explants confronted to superficial layer or C3a-coated beads and followed by time-lapse microscopy movies could be done to answer this question.

In the ectoderm, C3 display a unique, punctuate expression pattern displaying higher levels in the dorsal than in the ventral half of the embryo (Figure 3.1). This does not recapitulate the C3 expression pattern observed in other migratory cell populations such as the neural crest (McLin et al., 2008 and non shown data). This breakdown of symmetry or homogeneity has also been shown (among others ectodermal markers) for the ion transport genes in larval *Xenopus* (Quigley et al., 2011) and NeuroD1/Beta2 (Sharma et al., 199) and the keratin genes (for more about the chemical basis of differential expression pattern see Turing, 1952). In the case of C3, the expression levels in the ventral and dorsal regions were compared to the average expression in the whole animal cap, showing an approximate 50% reduction in the ventral region and an approximate 50% increase in the dorsal region. Interestingly, thinning in dorsal regions is significantly higher than in ventral regions (data not shown). This asymmetry might contribute to known dorso-ventral differences in gastrulation of *Xenopus* embryos (Bauer et al., 1994) suggesting that there might be other cell-restricted factor acting in conjunction with C3 to regulate differential C3 expression thereby controlling radial intercalation and thinning of the ectoderm.

It has been demonstrated that cell divisions plays a key role in regulating the first stages of ectoderm epiboly in *Xenopus* (Keller, 1978; Keller 1980). No differences in number of cell divisions were observed in CoMO when compared with C3MO or C3aRMO injected embryos (data not shown). Even though we

cannot completely rule out an undetected contribution of cell division, it is very unlikely that it could explain the strong impairment of epiboly observed in C3 and C3aR morphants embryos.

The experiments shown in Figure 3.2d-g demonstrate that C3aR is required in the ectoderm for proper movement of ectodermal cells and expansion of the superficial ectoderm. C3aR expression is almost undetected in superficial cells and we did not detect any behaviour phenotype in C3aRMO-injected superficial cells in our chemotaxis assays when seeded together with deep cells (data not shown). Therefore, even though we cannot rule out a minor contribution of C3aR in superficial cells, we believe that the reduction on ectoderm expansion and movement is due to C3aR- mediated effect in cells of the deep layer.

Different to the neural crest cells, deep cells do not express both C3a and C3aR but only C3aR (Figure 3.1). Depletion of C3a or C3aR in the neural crest inhibits cell migration by inducing enhanced cell dispersion and decreased cohesion of the cell group (Carmona-Fontaine et al., 2012). This phenotype is not observed when C3a/C3aR is depleted in the superficial and deep layer respectively (movies used to make Figure 3.4) suggesting that mutual cell attraction does not account for the role of C3a in regulating cell migration of the deep cells. Whereas C3a is produced in the Neural Crest cells to promote co-attraction, C3a is produced by the superficial layer of the ectoderm to promote chemotaxis of the deep cells.

In zebrafish, it has been shown that completion of normal epiboly of deep cells requires E-cadherin in a cell-autonomous fashion (Kane et al., 2005). E-cadherin is required for radially intercalated cells to integrate properly into their new location (Kane et al., 2005; partially reviewed in Walck-Shannon and Hardin, 2014). The deep cell epiboly phenotype associated with *cdh1* mutant embryos and morphants is attributed to defects in radial intercalation in the epiblast (Kane et al., 2005; Montero et al., 2005).

In *Xenopus*, Levine and colleagues showed that the integrity of the presumptive ectoderm is disrupted upon expression of a dominant negative form of E-cadherin (Levine et al., 1994). On this work, even when the truncated

form is injected into both cells of 2-cell embryos, the defects still appear to be restricted to the ectoderm. The *in vitro* experiments shown in Figure 3.3. suggest that C3aRMO injected cells are indistinguishable from CoMO injected cells for their ability to bind FN, deep layer or superficial layer. However, whether E-cadherin depletion disrupts epiboly remains still unknown; mainly because the severity of the phenotype in E- cadherin depleted embryos is so high that it is difficult to address any other phenotype beyond the holes that appears in the pigmented superficial layer (Levine et al., 1994). What is clear nonetheless is that even though we cannot completely rule out that C3aR might have an undetectable effect on cell adhesion, it is unlikely that it can explain the strong effect in epiboly and cell motility of the ectoderm cells observed in embryos where C3aR has been depleted.

In zebrafish, before epiboly begins, deep cells become motile exhibiting blebs and moving in random directions until the onset of epiboly when cells move radially outwardly (Kimmel and Warga 1987; Wilson et al., 1995). Before, epiboly, the deep cells merely appear to simply fill in the space between the yolk cells and the enveloping layer. Interestingly, during epiboly the blastoderm thins very uniformly suggesting a tight control in cell movement for deep cells to perform a precise thinning of the blastoderm. However, it is currently unclear whether deep cells move actively or passively; regardless of whether deep cell move actively or passively, cell motility is a permissive requirement for epiboly to undergo (Lepage and Bruce., 2010). The prevailing model to explain epiboly in zebrafish is based on differential adhesiveness between interior and exterior epiblast cells due to differential expression of E-cadherin (Petridou 2013; Kane 2005). Although the support for this graded expression of E-cadherin has turned out controversial (Song et al., 2013), there is strong evidence that the dynamics of E-cadherin is essential for epiboly in zebrafish (Kane et al., 2005; Arboleda-Estudillo et al., 2010; Babb et al., 2004). This dynamic cell adhesion is consistent with our computational-based model (data not shown) where deep cells slide past the superficial cells, similar to what has been proposed for the migration of prechordal plate mesendoderm, germ and border cells (Ulrich et al., 2009; Kardash et al., 2010; Ulrich et al., 2005; Cai et al., 2014). The chemotaxis-based model presented in this work could apply for teleost epiboly

but its identification may be hampered by the abundance of C3 genes in fish (Forn-Cuní et al., 2014) (discussed in Cobo and Szabo, submitted).

In *Xenopus*, fibronectin lining the blastocoel roof is essential for deep cell intercalation behaviours at gastrulation (Marsden and DeSimone, 2001). Embryos where fibronectin has been depleted display a thicker blastocoel roof; that thickening is not due to an increase in cell proliferation because no increase in the number of mitotic indices in this population was observed in the absence of a FN matrix. Fibronectin was also observed to be required for blastocoel roof deep cell intercalation and this effect was mediated by α5β1 integrin (Marsden and DeSimone, 2001). Following this observation, one could argue that C3a might be involved in fibronectin or integrin dynamics and that would affect migration of deep cells and epiboly of the ectoderm. Even though there is no evidence in immune cells for the role of C3a or C3aR in regulating FN deposition or involvement in integrin dynamics we can never exclude that it is the case for *Xenopus* ectoderm cells. Following these questions, immunofluorescence experiments against FN in CoMO and C3aRMO injected embryos would help us to check whether FN levels are compromised upon C3aR knockdown. If FN levels are not affected, then the C3a-mediated chemotaxis will denote an alternative mechanism, non based on FN expression (and eventually attachment to fibronectin). It would be still possible that fibronectin played a role in polarising the deep cells or regulating orientated cell division, which is known tho play an important role in epiboly (Marsden and DeSimone, 2001). On the other hand, one of the things that remain still unknown is which is the molecular mechanism downstream of C3aR. C3a signaling through phosphorylated Akt has been demonstrated for murine natural regulatory T cells (Kwan et al., 2013). However, given the above-mentioned role of integrins in regulating radial cell intercalation in *Xenopus* and the requirement of C3aR for deep cell migration, it would be interesting to check whether integrin is involved in the C3a-mediated chemotaxis of deep layer. Integrins overactivation experiments in the context of C3aRMO knockdown, both *in vivo* and *in vitro*, would be helpful to address whether the integrins are key mediators of C3a-driven chemotaxis of deep layer cells during epiboly of the animal cap.

Regarding E-cadherin, except for its role in zebrafish, no molecular characterisation of the role E-cadherin in deep ectodermal cells of *Xenopus* gastrulation has been demonstrated. Early reports showed that E-cadherin is mainly expressed in superficial layer of the ectoderm but in the deep cells only at very low levels (Choi and Gambier, 1989, Angres et al., 1991; Nandadasa et al., 2009). In the last years, however, some studies have reported the relationship between C3a and cell adhesion proteins, in particular E-cadherin. In 2009, Liu and colleagues (Liu et al., 2011) showed that upon C3a stimulation, E-cadherin expression is downregulated, thereby promoting a cellular transformation. C3a has also been shown to mediate E-cadherin downregulation in Renal Tubular Epithelial cells and promotes an epithelial-to-mesenchymal transition in these cells (Tang et al., 2009). Expression analysis of proteins of the caherin-based adherence junction family in C3aRMO injected deep layer cells would be helpful to understand whether upon C3aR depletion there is a de-regulation of cell adhesion proteins that could take part in the chemotaxis phenotype that we have reported.

In 1992, Keller showed that the involution of the marginal zone and the blastopore closure by the involuting marginal zone can occur without the epiboly-driven pushing force and the convergence extension of the non-involuting marginal zone and animal cap. When the pressure of the blastocoel roof is eliminated through the removal of the epidermis (without eliminating the mechanics of the tissue) the blastopore closure was not affected. The apparent controversy between these observations and what we have observed in the embryos injected with either C3 or C3aRMO can be explained by the fact that tissues have both active and passive biophysical roles in embryonic morphogenesis, therefore, removal of a tissue might not be equivalent to the same tissue being present but in an active or abnormal physiological condition (Keller 1992). Our results suggest that although C3a/C3aR-mediated epiboly of the ectoderm is required for the proper timing during blastopore closure, the timing of epiboly is not required for the final blastopore closure as embryos delayed on blastopore closure eventually manage to close the blastopore at later stages (data not shown).

In conclusion, several novel findings are presented in this thesis. Here we found for the first time that C3a and C3aR are expressed in the superficial and deep layer respectively (Figure 3.1). Combinatorial tissue experiments of deep layer and superficial layer explants show that the deep cells move collectively as a group toward the superficial layer (Figure 3.2). Moreover, we also demonstrate that C3a is sufficient to induce chemotaxis of the deep layer (Figure 3.3) and that depletion of C3 in the superficial layer or C3aR in the deep layer impairs chemotaxis of the deep cells toward superficial layer explants (Figure 3.4). Furthermore, we found that C3 (data not shown) and C3aR expression in the ectoderm is required for ectodermal epiboly (Figure 3.5) and that impairment of epiboly in the ectoderm is required for proper timing of the blastopore closure during gastrulation (Figure 3.6). However, due to its complexity, it is then clear that a deeper study of how intercalation programmes are activated will be fundamental to fully understand their potential in treating human patients (Walck-Shannon et al., 2014).

.

Part V: References

1. Al-Sharif WZ, Sunyer JO, Lambris JD, Smith LC. Sea urchin coelomocytes specifically express a homologue of the complement component C3. *Journal of Immunology.* **162**(5):3105 (1999).

2. Bauer, D.V., Huang, S and Moody, S.A. The cleavage stage origin of Spemann´s Organizer: analysis of the movement of blastomere clones before and during gastrulation in *Xenopus. Development* **120**,1179-82 (1994).

3. Bellairs R. The primitive streak. *Anatomy and Embryology*, **174**, 1-14. 1986

4. Bensch, R. Song, S., Ronneberger, O and Driever, W. Non-directional radial intercalation dominates deep cell behaviour during zebrafish epiboly. *Biology Open.* **2**, 845-54 (2013).

5. Boucaut C, Darribere T, Shi de Li, Boulekbache H, Thiery P. Evidence for the role of fibronectin in amphibian gastrulation. *Journal of embryology and experimental morphology.* **89**, Supplement: 211-227 (1985).

6. Breau MA, Wilkinson DG, Xu Q. *Proceedings of the national Academy of Sciences.* **42,** 16892-7 (2013).

7. Cai D. Mechanical Feedback thorough E-cadherin Promotes Direction Sensing during Collective Cell Migration. *Cell.* **157**, 1146-1159 (2014).

8. Canning DR and Stern C. Changes in the expression of the carbohydrate epitope Hnk-1 is associated with mesoderm induction in the chick embryo. *Development.* **104**, 643-655 (1988).

9. Carlos Carmona-Fontaine, Helen K. Matthews, Sei Kuriyama, Mauricio Moreno, Graham A. Dunn, Maddy Parsons, Claudio D. Stern & Roberto Mayor. Contact inhibition of locomotion in vivo controls neural crest directional migration. *Nature.* **456**, 957-961 (2008).

10. Carmona-Fontaine C, Theveneau E, Tzekou A, Tada M, Woods M, Page KM, Parsons M, Lambris JD, Mayor R. Complement fragment C3a controls mutual cell attraction during collective cell migration. *Developmental Cell*. **21(6)**:1026-37 (2011).

11. Carney TJ, Stemmler M, Koschorz B, Amsterdam A, Schwarz H, Hammerschmidt M. The Epithelial Cell Adhesion Molecule EpCAM is required for Epithelial Morphogenesis and Integrity during Zebrafish Epiboly and Skin Development. *Public Library of Science Genetics*. **5(7)** (2009).

12. Carroll, T.J and Yu J. The kidney and planar cell polarity. *Current Topics of Developmental Biology*. **28**, 185-212 (2012).

13. Chalmers, A.D, Strauss, B., Papalopulu, N. Oriented cell divisions asymmetrically segregate aPKC and generate cell fate diversity in the early *Xenopus* embryo. *Development* 130, 2657-2668 (2003).

14. Damm, E. W. and Winklbauer, R. PDGF-A controls mesoderm cell orientation and radial intercalation during *Xenopus* gastrulation. *Development* 138, 565-75 (2011).

15. Del Rio-Tsonis K, Tsonis PA, Zarkadis IK, Tsangas AG, Lambris JD. Expression of the third component of complement, C3, in regenerating limb blastema cells of urodeles. *Journal of Immunology*, **161**, 6819-6824 (1998).

16. Drews U. Cholinesterase in embryonic development. *Progress in Histochemistry and Cytochemistry*. **7**, 1-52 (1975).

17. Eyal-Gilaldi H, Kochav S. From cleavage to primitive streak formation: a complementary normal table and a new look at the first stages of the development of the chick. General morphology. *Developmental Biology*. **49**, 321-337 (1976).

18. Forn-Cuní G, Reis ES, Dios S, Posada D, Lambris JD, Figueras A, Novoa B. The evolution and appearance of C3 duplications in fish originate an exclusive teleost C3 gene form with anti-inflammatory activity. *Public Library of Sciences, PLoS One*. J, **6,**, e99673 (2014).

19. Fukui, A., Goto, T., Kitamoto, J., Homma, M. & Asashima, M. SDF-1 alpha regulates mesendodermal cell migration during frog gastrulation. *Biochemical and Biophysical Research Communications*. 354, 472–477 (2007).

20. Gasque P, Morgan BP. Complement regulatory protein expression by a human oligodendrocyte cell line: cytokine regulation and comparison with astrocytes. *Immunology*. **89**, 338-47 (1996).

21. Gasque P, Thomas A, Fontaine M, Morgan BP. Complement activation on human neuroblastoma cell lines in vitro: route of activation and expression of functional complement regulatory proteins. *Journal of Neuroimmunology*. **66**, 29-40 (1996).

22. Gasque, P., Ischenko, A., Legoedec, J., Mauger, C., Schouft, M.T., Fontaine, M. Expression of the complement classical pathway by human glioma in culture. *Journal of Biological Chemistry*. **268**, 25068–25074 (1993).

23. Gilbert SF. Developmental Biology. **2007**, **2008**, **2010** editions.

24. Goode, B.L., Eck, M.J. Mechanism and functions of formins in the control of actin assembly. *Annual Review of Biochemistry*. **76**, 593-627 (2007).

25. Gräper L. Die Primitiventwicklung des Hünchens nach stereokinematographischen Untersuchungen, kontrolliert durch vitale Farbmarkierung und verglichen mit der Entwicklung anderer Wirbeltiere. Archiv der Entwicklungmechanik der Organismen. **116**, 382-429 (1929).

26. Gray, R., Roszko, I and Solnical-Krezel, L. Planar cell polarity: coordinating morphogenetic cell behaviour with embryonic polarity. *Developmental Cell.* **21**, 120-131 (2011).

27. Gutzmer R, Lisewski M, Zwirner J, Mommert S, Diesel C, Wittmann M, Kapp A, Werfel T. Human monocyte-derived dendritic cells are chemoattracted to C3a after up-regulation of the C3a receptor with interferons. *Immunology.* **4**, 435-43 (2004).

28. Harrison, Lionel G. (2011). The Shaping of Life: The Generation of Biological Pattern. Cambridge University Press. p. **206**. ISBN 978-0-521-55350-6.

29. Hartmann K, Henz BM, Krüger-Krasagakes S, Köhl J, Burger R, Guhl S, Haase I, Lippert U, Zuberbier T. C3a and C5a stimulate chemotaxis of human mast cells. *Blood.* **8**, 2863-70 (1997).

30. Haynes T, Luz-Madrigal A, Reis ES, Echeverri Ruiz NP, Grajales-Esquivel E, Tzekou A, Tsonis PA, Lambris JD, Del Rio-Tsonis K. Complement anaphylatoxin C3a is a potent inducer of embryonic chick retina regeneration. *Nature Communications.* **4**, 2312 (2013).

31. Honczarenko M, Ratajczak MZ, Nicholson-Weller A, Silberstein LE. Complement C3a enhances CXCL12 (SDF-1)-mediated chemotaxis of bone marrow hematopoietic cells independently of C3a receptor. *Journal of Immunology.* **6**, 3698-706 (2005).

32. Hossain, M.J., Whelan, P.F., Czirók, A. and Ghita, O. An active particle-based tracking framework for 2D and 3D time-lapse microscopy images. *Conf, Proc. IEEE Eng. Med. Biol. Soc*, 6613-8 (2011).

33. Huang CF, Lira C, Chu K, Bilen MA, Lee YC, Ye X, Kim SM, Ortiz A, Wu FL, Logothetis CJ, Yu-Lee LY, Lin SH. Cadherin-11 increases migration and invasion of prostate cancer cells and enhances their interaction with osteoblasts. *Cancer Research.* **11**, 4580-9 (2010).

34. Jansen BJ, Christodoulidou A, McCarthy A, Lambris JD, Gros P. Structure of C3b reveals conformational changes that underlie complement activity. *Nature.* **444**, 213-6 (2010).

35. Janssen BJ, Huizinga EG, Raaijmakers HC, Roos A, Daha MR, Nilsson-Ekdahl K, Nilsson B, Gros P. Structures of complement component C3 provide insights into the function and evolution of immunity. *Nature.* 437, 505-11 (2005).

36. Kane, D. A. and Kimmel, C. B. The zebrafish midblastula transition. *Development* **119**, 447-456 (1993).

37. Kane, D. A., McFarland, K. N. and Warga, R. M. Mutations in half baked/Cdh1 block cell behaviors that are necessary for teleost epiboly. *Development* 132: 1105-1116 (2005).

38. Kardash, E. A role for Rho GTPases and cell-cell adhesion in single-cell motility in vivo. *Nature Cell Biology*. **12**, 11-47 (2010).

39. Keller RE. The cellular basis of epiboly: an SEM study of deep-cell rearrangement during gastrulation in Xenopus laevis. *Journal of Embryology and Experimental Morphology*. **60**, 201-34 (1980).

40. Keller, R., Davidson, L.A., and Shook, D.R. How are we shaped: the biomechanics of gastrulation. *Differentiation*. **71**, 171-205 (2003).

41. Keller, RE. Mechanisms of elongation in embryogenesis. *Development*. **133**, 2291-2302 (2006).

42. Kemper C, Atkinson JP, Hourcade DE. Properdin: emerging roles of a pattern-recognition molecule. *Annual Review of Immunology*. **28**, 131-155 (2010).

43. Kimmel, C. B., Warga, R. M. and Schilling, T. F. Origin and organization of the zebrafish fate map. *Development*. **108**, 581-594 (1990) .

44. Kimura, Y. *et al*. Expression of complement 3 and complement 5 in newt limb and lens regeneration. *Journal of Immunology*. **170**, 2331–2339 (2003).

45. Kishore U, Reid KB. C1q: structure, function, and receptors. *Immunopharmacology*. **49**, 159-70 (2000).

46. Kwan WH, van der Touw W, Paz-Artal E, Li MO, Heeger PS. Signaling through C5a receptor and C3a receptor diminishes function of murine natural regulatory T cells. *Journal of Experimental Medicine.* **210**, 257-68 (2013).

47. Lachnit, M., KUR, E. and Driever, W. Alterations of the cytoskeleton in all three embryonic lineages contribute to the epiboly defect of Pou5f1/Oct4 deficient MZspg zebrafish embryos. *Developmental Biology* 315: 1-17 (2008).

48. Ladwein, M. and Rottner, K. On the Rho'd: the regulation of membrane protrusions by Rho-GTPases. *FEBS Lett* **582**, 2066-2074 (2008).

49. Lai SL, Chan TH, Lin MJ, Huang WP, Lou SW, Lee SJ. Diaphanous-related formin 2 and profilin I are required for gastrulation cell movements. *Public Library of Science, PLos One.* **3(10)** (2008).

50. Lambris JD, Sahu A, Wetsel R. The chemistry and biology of C3,C4, and C5. In: Volanakis JE, Frank M, eds. The human complement system in health and disease. New York: Marcel Dekker Inc; 1998. p. 83–118.

51. Latimer A, Jessen JR. Extracellular matriz assembly and organization during Zebrafish gastrulation. *Matrix Biology.* **29(2)**, 89-96 (2010).

52. Lepage SE, Bruce AE. Zebrafish epiboly: mechanics and mechanisms. *International Journal of Developmental Biology*; **54**, 1213-1228 (2010).

53. Leskow FC, Holloway BA, Wang H, Mullins MC, Kazanietz MG. The zebrafish homologue of mammalian chimerin Rac-GAPs is implicated in epiboly progression during development. *Proceeding of National Academic Sciences USA.* **103**, 5373-8 (2006).

54. Lienkamp, S et al. Vertebrate kidney tubules elongate using a planar cell polarity-dependant, rosette-based mechanism of convergence extension. *Nature Genetics.* **44**, 1382-1387 (2012).

55. Liu F, Gou R, Huang J, Fu P, Chen F, Fan WX, Huang YQ, Zang L, Wu M, Qiu HY, Wei DP. Effect of anaphylotoxin C3a, C5a on the tubular epithelial-myofibroblast transdifferentiation in vitro. *Chinese Medical Journal (English).* **124**, 4039-45 (2011).

56. Longo D., Peirce S., Skalak TC., Davidson L., Marsden M., Dzamba B., DeSimone DW. Multicellular computer simulation of morphogenesis: blastocoel roof thinning and matrix assemby in *Xenopus laevis. Developmental Biology*, **271**, 210-222 (2004).

57. Lunde, K., Belting, H. G. and Driever, W. Zebrafish pou5f1/pou2, homolog of mammalian Oct4, functions in the endoderm specification cascade. *Current Biology.* **14**, 48-55 (2004).

58. McMahon A, Supatto W, Fraser SE, Stathopoulos A. *Science.* **332**, 1546-50 (2008).

59. Málaga-Trillo, E., Solis, G. P., Schrock, Y., Geiss, C., Luncz, L., Thomanetz, V. and Stuermer, C. A. Regulation of embryonic cell adhesion by the prion protein. *Public Library of Sciences Biology.* **7**: e55 (2009).

60. Marsden M, DeSimone DW. Regulation of cell polarity, radial intercalation and epiboly in Xenopus: novel roles for integrin and fibronectin. *Development.* **128**, 3635-47 (2001).

61. McGrath FD, Brouwer MC, Arlaud GJ, Daha MR, Hack CE, Roos A. Evidence that complement protein C1q interacts with C-reactive protein through its globular head region. *Journal of Immunology.* **176**, 2950-7 (2006).

62. McLin VA, Hu CH, Shah R, Jamrich M. Expression of complement components coincides with early patterning and organogenesis in Xenopus laevis. *International Journal of Developmental Biology.* **52,** 1123-1133 (2008).

63. Mastellos D, Lambris JD. Complement: more than a 'guard' against invading pathogens? *Trends in Immunology.* **10**, 485-91 (2002).

64. May-Simera, H and Kelley, M.W. Planar cell polarity in the inner ear. *Current Topics in Developmental Biology.* **101**, 111-140 (2012).

65. Montero, J. A., Carvalho, L., Wilsch-Brauninger, M., Kilian, B., Mustafa, C. and Heisenberg, C. P. Shield formation at the onset of zebrafish gastrulation. *Development* **132**: 1187-1198 (2005).

66. Morgan BP, Gasque P. Expression of complement in the brain: role in health and disease. *Immunoligy Today*. **17**, 461-6 (1996).

67. Nishio, S. Loos of oriented cell division does not initiate cyst formation. *Journal of the American Society of Nephrology*. **21**, 295-302 (2010).

68. Pangburn MK, Müller-Eberhard HJ. Initiation of the alternative complement pathway due to spontaneous hydrolysis of the thioester of C3. *Annals of the New York Academy of Sciences*. **421**, 291-8 (1983).

69. Petridou NI, Stylianou P, Skourides PA. A dominant-negative provides new insights into FAK regulation and function in early embryonic morphogenesis. *Development*. **140**, 4266-76 (2013).

70. Psychoyos D, Stern CD. Fates and migratory routes of primitive streak cells in the chick embryo. *Development*. **122**, 1523-1534 (1996).

71. Quigley, I, Jennifer L. Stubbs and Chris Kintner. Specification of ion transport cells in the *Xenopuos* larval skin. *Development*. **138**, 705-714 (2011).

72. Reim, G., Mizoguchi, T., Stainier, D. Y., Kikuchi, Y. and Brand, M. The POU domain protein spg (pou2/Oct4) is essential for endoderm formation in cooperation with the HMG domain protein casanova. *Developmental Cell*. **6**, 91-101 (2004).

73. Ricklin D, Hajishengallis G, Yang K, Lambris JD. 2010. Complement: a key system for immune surveillance and homeostasis. *Nature Immunology*. **11**, 785-97 (2010).

74. Rogers CA, Gasque P, Piddlesden SJ, Okada N, Holers VM, Morgan BP. Expression and function of membrane regulators of complement on rat astrocytes in culture. *Immunology*. **88**:153-61 (1996).

75. S. K. Law and A. W. Dodds. The internal thioester and the covalent binding properties of the complement proteins C3 and C4. *Protein Science*. **6**, 263-274 (1997).

76. Sacks SH. Complement fragments C3a and C5a: the salt and pepper of the immune response. *European Journal of Immunology*. **40**, 668-70 (2010).

77. Sahu A, Lambris JD. Structure and biology of complement protein C3, a connecting link between innate and acquired immunity. *Immunology Review*. **180**, 35-48 (2001).

78. Schepis A, Sepich D, Nelson WJ. αE-catenin regulates cell-cell adhesion and membrane blebbing during zebrafish epiboly. *Development*. **139**, 537-46 (2012).

79. Schraufstatter IU, Discipio RG, Zhao M, Khaldoyanidi SK. C3a and C5a are chemotactic factors for human mesenchymal stem cells, which cause prolonged ERK1/2 phosphorylation. *Journal of Immunology*. **182**(6), 3827-36 (2009).

80. Sharma A., Moore M., Marcora E., Jacqueline E., Lee, Qiu Y., Samaras, S, and Stein, R. The NeuroD1/Beta2 Sequences Essential for Insulin Gene Transcription Colocalize with Those Necessary for Neurogenesis and p300/CREB Binding Protein Binding. *Molecular Cell Biology*. **19**, 704-713 (1999).

81. Solnica-Krezel L and Driver W. Microtubule arrays of the zebrafish yolk cell: organization and function during epiboly. *Development*. **120**, 2443-55 (1994).

82. Song S, Eckerle S, Onichtchouk D, Marrs JA, Nitschke R, Driever W. Pou5f1-dependent EGF expression controls E-cadherin endocytosis, cell adhesion, and zebrafish epiboly movements. *Developmental Cell*. **24**, 486-501 (2013).

83. Smith JC, Symes K, Hynes R.O, DeSimone D. Mesoderm induction and the control of gastrulation in *Xenopus lavis*: the roles of fibronectin and integrins. *Development*. **108**, 229-238 (1990).

84. Stevens B, Allen NJ, Vazquez LE, Howell GR, Crhristopherson KS, Nouri N, Micheva KD, Mehalow AK, Huberman AD, Stafford B, Sher A, Litke AM, Lambris JD, Smith S, John SW, Barres BA. The classical complement cascade mediates CNS synapse elimination. *Cell*. **131,** 1164-78 (2007).

85. Strainic MG, Liu J, Huang D, An F, Lalli PN, Muqim N, Shapiro VS, Dubyak GR, Heeger PS, Medof ME. Locally produced complement fragments C5a and C3a provide both costimulatory and survival signals to naive CD4+ T cells. *Immunity*. **28**, 425-35 (2008).

86. Strainic MG, Shevach EM, An F, Lin F, Medof ME. Absence of signaling into CD4^{+} cells via C3aR and C5aR enables autoinductive TGF-β1 signaling and induction of Foxp3^{+} regulatory T cells. *Nature Immunology*. **14**, 162-71 (2013).

87. Sunyer, J. O., Zarkadis, I. K. & Lambris, J. D.Complement diversity: a mechanism for generating immune diversity? *Immunology Today* . **19**, 519-523 (1998).

88. Tada M and Kai M. Planar cell polarity in coordinated and directed movements. *Current Topics in Developmental Biology*. **101**, 77-110 (2012).

89. Tang, Z., Lu, B., Hatch, E., Sacks, SH., Sheerin N. C3a Mediates Epithelial-to-Mesenchymal Transition in Proteinuric Nephropathy. *Journal of the American Society of Nephrology.* **20**, 593-603 (2009).

90. T. A. McGeady, P. J. Quinn, E. S. FitzPatrick, M. T. Ryan. *Veterinary Embryology*.

91. Theveneau E, Steventon B, Scarpa E, Garcia S, Trepat X, Streit A, Mayor R. Chase-and-run between adjacent cell populations promotes directional collective migration. *Nature Cell Biology*. **15**, 763-72 (2013).

92. Thirusittmpalam, K., Hossain, M.J., Ghita, O. and Whelan, P.F. A novel Framework for Cellular Tracking and Mitosis Detection in Dense Phase Contrast Microscopy Images, IEEE Trans, Biomed, Heal. Informatics **17**, 3, 3 642-653 (2013).

93. Turing A.M. The chemical Basis of Morphogenesis. Phylosophical Transactions of the Royal Society of London. Series B. Biological Sciences, Vol 237, No. **641**, 37-72 (1952).

94. Ulrich F et al., Wnt 11 funtions in gastrulation by controlling cell cohesion through Rab5c and E-cadherin. *Developmental Cell*. **9**, 555-564 (2005).

95. Ulrich F and Heisenberg, C. P. Trafficking and cell migration. *Traffic.* **10**, 811-8 (2009).

96. Vakaet L. The initiation of gastrular ingression in the chick blastoderm. *American Zoologist*. **24**: 555-562 (1984).

97. Voiculescu O, Bertocchini F, Wolpert L, Keller RE, Stern CD. The amniote primitive streak is defined by epithelial cell intercalation before gastrulation. *Nature*. **449**, 1049-52 (2007).

98. Voiculescu O, Bodenstein L, Lau IJ, Stern CD. Local cell interactions and self-amplifying individual cell ingression drive amniote gastrulaion. *Elife*. 3:e01817 (2014).

99. Walck-Shanon and Jeff Hardin. Cell intercalation from top to bottom. *Nature reviews*. **15,** 34-48 (2014).

100. Wallingford, J. Planar cell polarity and the developmental control of cell behaviour in vertebrates. *Annual Review of Cell and Developmental Biology*. **28**, 627-653 (2012).

101. Warga, R. M. and Kimmel, C. B. Cell movements during epiboly and gastrulation in zebrafish. *Development*. **108**, 569-580 (1990).

102. Wei, Y and Mikawa, T. Formation of the avian primitive streak from spatially restricted blastoderm: evidence for polarized cell division en the elongating streak. *Development*. **127**, 87-96 (2000).

103. Wessel, G. M. and McClay, D. R. Sequential expression of germ-layer specific molecules in the sea urchin embryo. *Developmental Biology*. **111**, 451-463 (1985).

104. Wetzel R. Untersuchungen am Huhnchen. Die Entwicklung des Keims wahrend der erste beiden Bruttage. *Archiv der Entwicklungmechanik der Organismen*. **119**, 188-321 (1929).

105. Wilson, P and Keller, R. Cell rearrangement during gastrulation of *Xenopus:* direct observations of cultured explants. *Development*. **11**, 289-300 (1991).

106. Wilson, E. T., Cretekos, C. J. and Helde, K. A. Cell mixing during early epiboly in the zebrafish embryo. *Developmental Genetics*. **17**, 6-15 (1985).

107. Zwirner J, Werfel T, Wiken H, Theile E and Gotze O. Complement C3a but not C3adesArg is a chemotaxin for the mouse macrophage cell line J774. *European Journal of Immunology*. **28**, 1570-1577 (1998).